Geomorphology 492 (2026) 110054

Contents lists available at ScienceDirect

Geomorphology

journal homepage: www.journals.elsevier.com/geomorphology

High alpine preglacial caves modified by glacial processes and late condensation-corrosion in the Scerscen Valley (Valmalenco, Western Alps, Italy)

Philippe Audra [a], Jo De Waele [b,c,*], Alessandro Uggeri [d], Didier Cailhol [e], Ilenia M. D'Angeli [c], Adriano Fiorucci [f], Ivano Foianini [g], Samuele Foianini [g], Régis Braucher [h], Mauro Inglese [i], Andrea Maconi [i], Felicita Spreafico [j], Marco Barile [d], Cristina Carbone [k], Paola Tognini [i]

[a] Université Côte d'Azur, Polytech'Lab - UPR 7498, 930 route des Colles, 06903, Sophia-Antipolis, France
[b] Dipartimento di Scienze Biologiche, Geologiche ed Ambientali BIGEA, Università di Bologna Alma Mater Studiorum, Via Zamboni 67, Bologna, Italy
[c] Istituto Italiano di Speleologia, Via Zamboni 67, Bologna, Italy
[d] Idrogea Servizi s.r.l., Gruppo Speleologico CAI Varese, Italy
[e] Traces Laboratory, University Toulouse Jean Jaurès, France
[f] Dipartimento di Ingegneria dell'Ambiente, del Territorio e delle Infrastrutture (DIATI), Politecnico di Torino, Corso Duca degli Abruzzi 24, Torino, Italy
[g] Istituto Valtellinese di Mineralogia "Fulvio Grazioli, Sondrio, Italy
[h] CNRS, IRD, INRAE, CEREGE, Aix Marseille University, Aix-en-Provence, France
[i] Gruppo Grotte Milano CAI-SEM, Federazione Speleologica Lombarda, Milano, Italy
[j] Speleo Club CAI Erba, Italy
[k] Dipartimento di Scienze della Terra, dell'Ambiente e della Vita, University of Genua, Corso Europa 26, Genova, Italy

ARTICLE INFO

Keywords:
Speleogenesis
Alpine glaciers
Geomorphology
Cosmogenic burial dating
Hydrogeology

ABSTRACT

The Scerscen Valley (western Italian Alps) is home to caves at an altitude of around 2600 m, opening close to the edge of a glacier. The aim of the research as part of a multi-disciplinary project was to reconstruct the evolution of the caves related to the geological and paleo-environmental evolution of the area and to evaluate the role of some of the most recent processes, such as condensation-corrosion and sediment deposition. We performed cosmonucleide burial dating, recorded morphology and micrometeorology, carried out mineralogical identification by XRD, and hydrogeology using dye tracing and physical and chemical analyses. The cosmonucleide dating of quartz pebbles showed that the Veronica Cave is the oldest, with deposits dated at 1.3 ± 0.4 Ma, and possibly even older. It certainly formed at a much lower altitude (approx. 1300 m a.s.l. or lower) during the Alpine uplift. The Morgana and Marsooi caves, given the smaller volume of their phreatic conduits (1/3 of Veronica), are possibly more recent, formed during interglacials and evolved close to a glacial body. The caves initiated in dolomitic marble under the influence of sulfuric acid speleogenesis (SAS) due to pyrite oxidation. The conduits were then enlarged dramatically under phreatic conditions. The caves have evolved since their preglacial formation, with phases of filling by fluvio-glacial sediments and unclogging. Water tracing and physico-chemical analysis attest to a well-karstified aquifer, with rapid water circulation (>20 m/h) and low temperatures (~2 °C), draining towards the main spring, "La Prediletta", located at the foot of the dolomitic marbles. Microclimatic records (cave temperature and humidity) show seasonal cycles of condensation and evaporation, influenced by air exchanges with the outside atmosphere. These processes contributed to the formation of secondary minerals by evaporation (gypsum, hydromagnesite…) and, above all, to the significant enlargement of passages by the retreat of walls with characteristic morphologies (facets and grooved walls). The Scerscen caves bear witness to a long geological and climatic history, from their formation before the Mid-Pleistocene ice ages to

* Corresponding author at: Dipartimento di Scienze Biologiche, Geologiche ed Ambientali BIGEA, Università di Bologna Alma Mater Studiorum, Via Zamboni 67, Bologna, Italy.

E-mail addresses: Philippe.AUDRA@univ-cotedazur.fr (P. Audra), jo.dewaele@unibo.it (J. De Waele), a.uggeri@idrogea.com (A. Uggeri), dcailhol@orange.fr (D. Cailhol), dangeli.ilenia89@gmail.com (I.M. D'Angeli), adriano.fiorucci@polito.it (A. Fiorucci), ifoianini@fondazionefojanini.it (I. Foianini), samuele.foianini@gmail.com (S. Foianini), braucher@cerege.fr (R. Braucher), cristina.carbone@unige.it (C. Carbone), paolatognini@iol.it (P. Tognini).

https://doi.org/10.1016/j.geomorph.2025.110054
Received 11 June 2025; Received in revised form 17 September 2025; Accepted 9 October 2025
Available online 14 October 2025

their present-day evolution. They offer valuable insights into karst processes in the high mountains, and interactions between glaciers and aquifers.

1. Introduction

Global warming is increasingly impacting our societies, with greater recurrence of extreme events (e.g., storms, river floods, extreme temperatures, bushfires) (Diffenbaugh et al., 2017), ocean acidification (i.e. impacting coral reefs) (Cornwall et al., 2021), and sea-level changes threatening coastal ecosystems (Hansen et al., 2023). This warming is twice to three times faster in mountain areas when compared to nearby lowland areas, with fast glacier retreat and the forecast of decreased water supply in the coming future (Pepin et al., 2022). Glacier retreat has increased dramatically worldwide in the last 20 years, and this is especially true for the glaciers in the European Alps (Bonardi et al., 2012; Hugonnet et al., 2021). This is not only confirmed by monitoring ice extensions using satellite images throughout the years (Sommer et al., 2020), but also by direct observations and modelling (Beniston et al., 2018).

Over 7000 caves are known in Lombardy, but only about 200 are found in the high Alps. The longest and deepest of these high alpine caves are located in the upper course of Valtellina and in Chiavenna Valley, where a few small karst areas exist, scattered in very high mountain zones. The Lombard Alps are therefore rather poor in caves, either for the scarce occurrence of carbonate formations and for the intense tectonic deformations affecting the rocks. Furthermore, reaching the karst areas and exploring these caves is rather challenging because of the remote high mountain locations. One of these high alpine cave areas is located near the Scerscen glacier.

Although the carbonate rocks of the Scerscen area just crop out along the slope as narrow stripes with limited lateral extension, and their high altitude does not appear to be favorable for the formation of caves, in 1986 a few entrances were discovered and explored (Tognini et al., 2017, 2024; Santagata et al., 2018). Further investigations in following years brought to the mapping of over 1 km of cave passages in three caves. These, and especially Morgana Cave, are characterized by the widespread presence of vermiculations (tortuous worm-like fine sediment decorations on the cave walls) of different colors, which were studied for their microbiological communities by Jurado et al. (2020). Morgana Cave is also home to a troglophile opilionid spider, *Dicranopalpus gesteinensis*, feeding on Diptera (mosquitoes) and their larvae (Dioli et al., 2012).

The study of the genesis and evolution of these caves is the main topic of this paper. After a presentation of the geomorphic and geological context, we report new geomorphological, hydrogeological and sedimentological data, including burial dating using the decay of previously in situ produced cosmogenic nuclides from quartz pebbles. We then discuss the origin of such type of caves surprisingly developed at such a high altitude, and their relationship with the glacier.

2. Geographical and geological setting

The Scerscen Valley is a lateral valley of Valmalenco, one of the main tributary valleys of Valtellina, which corresponds to the upper Adda catchment. Situated in the Central Italian Alps, Valtellina is developed along the most important Alpine fault line, the Insubric Line, thus separating the Alpine Domain from the South alpine one (Fig. 1).

In Valmalenco, Mallero River deeply cuts into the geological structure, thus creating a very good situation for studying and observing the very complex geology of the area. The Scerscen Valley joins Valmalenco from the north, cut by Lanterna Torrent, fed by the melting waters of the Lower and Upper Scerscen glaciers. The landscape is typically high mountain, with bare rocks scoured by glaciers: the study area is dominated by Piz Bernina, the highest mountain of the Central Alps (4048 m a.s.l), located at the border with Switzerland. To the north, the valley is cut by the Fex Valley, at the Italian-Swiss watershed. In 2003 the Scerscen Valley was declared Special Area of Conservation (SAC) for the beauty of the geological landscape and for the biodiversity of its high mountain ecosystem.

During the last maximum of the Little Ice Age (LIA, around the mid-19th century), this glacier covered an area of ca. 48 km^2, composed of a large ice mass from which three glacier tongues descended (Scerscen and Fellaria descending Southwards in Italy (Fig. 2), and a large glacier

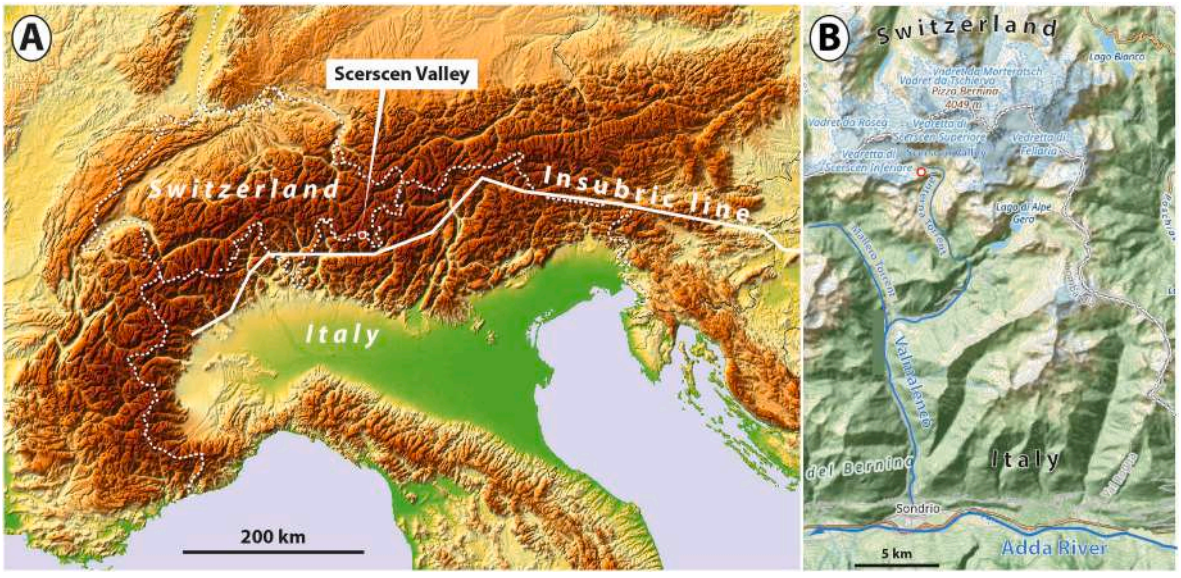

Fig. 1. (A) Terrain Map of the Alps. The Insubric line marks the boundary between Eurasian and Apulia plates, between Alpine and South alpine Domains (DTM after Imgur). (B) Closer view to Valmalenco, a right bank tributary of the Adda River in Valtellina. The Scerscen Valley is a tributary of Valmalenco draining the southern slopes of Piz Bernina, 4049 m (Background map from OpenStreetMap). The study area is indicated by a red target, the dotted line corresponds to the Swiss-Italian border.

on the Eastern Swiss side, now separated in many different "Vadret" (glaciers): Fex, Roseg, Tschierva, Morteratsch-Pers, etc., not shown in Fig. 2). Between 1850 and 1928, the Scerscen glacier tongue retreated over a linear distance of ca. 800 m, and in the following 30 years by another 1100 m (Galluccio and Scotti, 2022). Towards the end of the 1920s, an important stripe of white dolomitic marbles started to be freed from the ice at around 2500 m a.s.l., as clearly visible in some pictures taken by Alfredo Corti during the expedition organized by Giuseppe Nangeroni in 1929 (Fig. 3). These carbonates formed a nunatak for half a century, dividing several tributary ice tongues connecting the upper and lower parts of the Scerscen glacier. From 1950 onwards, this ridge eventually isolated the lower Scerscen glacier (with two glacier tongues) from the upper one. Both isolated glaciers continued their mass loss (the present situation is shown in Fig. 4), and by 2020 the upper Scerscen glacier (Vedretta di Scerscen) retreated over 3.2 km (ca. 45 m/a), and the western and southern glacier tongues of the lower Scerscen glacier by 3.5 and 2.9 km (ca. 50 and 41 m/a), respectively (Galluccio and Scotti, 2022). The Equilibrium Line Altitude (ELA) is presently close to 3000 m a.s.l.

The geological setting of Valmalenco is very complex (Montrasio, 1991; Montrasio et al., 2004): at least eight different Alpine tectonic sheets (nappes) are thrusted one over the others in this area (Fig. 5). After the Hercynian orogenesis (ca. 300 Ma), the pre-alpine paleogeography was characterized by a continental crust covered by a shallow sea (Helvetic-Dauphinois and Ultrahelvetic Domains) to the north, getting deeper to the south (Outer Penninic Domain), the oceanic crust of the Piedmont-Ligurian Ocean (which will later form the Alpine Ophiolite belt) and its sedimentary cover (Inner Penninic Domain), and, finally, to the south, the northern margin of the African plate (more precisely the Adria-Apulia microplate), which will be part of the Austrian alpine and South alpine Domains. During the Cretaceous, the oceanic crust was completely subducted southwards, and large slabs of the African plate cover overthrusted the "European" domains west- and northwestward (Austroalpine Domain). In the studied area, the deepest, northernmost nappe (Malenco-Forno Unit) belongs to the Penninic domain, representing the remnants of the ancient Piedmont-Ligurian oceanic crust separating the European plate to the north from the African Adria-Apulia microplate to the south, subducted southwards during the alpine orogenic phases: the Malenco-Forno Unit is mainly made up of the Malenco ultramafic ophiolitic complex (basalt, serpentinites and gabbros) and a thin layer of Jurassic-Cretaceous deep-sea metasediments (mica- and chlorite schists, quarzitic schists, quarzitic marbles). The upper nappes belong to the Austrian alpine Domain, thus representing the continental crust and the marine sedimentary cover of the Adria-Apulia plate. From the lower to the uppermost, the Austroalpine nappes cropping out in this area are the Margna, Sella, and Bernina nappes (Fig. 5). Each nappe is formed by a metamorphic basement (mainly paragneiss and micaschists, the so -called "Crystalline Basement") and intrusive rocks (granites, diorites and granodiorites, gabbros) of Hercynian (Variscan) and post-Hercynian age (pre-Alpine). In the lower nappes, such as Margna nappe, the sedimentary cover of the crystalline basement and of the intrusive rocks is still very well preserved, while it is almost completely obliterated by overthrusting in the uppermost Sella and Bernina nappes. The studied caves are found in the Margna nappe sedimentary cover.

The Margna nappe sedimentary cover is composed of Permo-Triassic quartzites and micaschists, Triassic dolostones (*Rauhwacken auct.*), Triassic dolomitic marbles, Jurassic (Lias-Dogger) calcitic-quarzitic marbles and dolomitic breccias, Jurassic-Cretaceous calc- and quartz schists with quartzite layers containing Mn and sulfidic mineralizations (Fig. 6A). The sedimentary sequence forms a very tight recumbent syncline fold, whose upper, overturned limb is eroded and partly covered by the Lower Scerscen Glacier: the sequence can be observed in the walls of Piz Tremogge, right at the border with Switzerland (Fig. 6B), and glacier retreat is causing larger portions of the fold to crop out (Fig. 4). The caves are almost entirely developed inside the Triassic dolomitic marbles, dipping N-NE towards the axial core of the fold, still ice-covered. To the south, the sedimentary cover is cut by vertical walls and by the Lanterna Torrent incision. In these walls, many small cave entrances have been found, cut by slope retreat, and small springs emerge from debris cones at the foot of the walls.

3. Methods

3.1. Petrography and mineralogy

Petrographic observations were carried out on thin sections placed under a Nikon Eclipse Ci-Pol binocular petrographic microscope equipped with a DS-Fi2-L3 digital camera at BiGeA department, University of Bologna.

Secondary mineral samples were taken and dried at room temperature for a few days. Mineralogical analyses used X ray powder diffraction

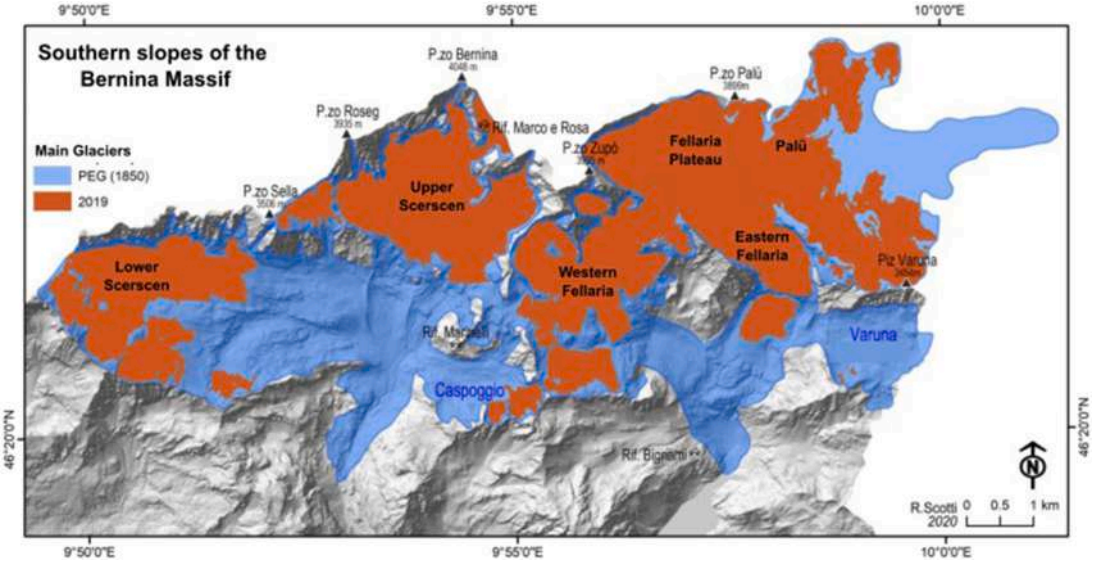

Fig. 2. Recent retreat of the glaciers of the Southern Piz Bernina area: LIA (PEG "Piccola Era Glaciale" 1850 in this figure) extent in mid-XIXth Century (in blue), and current extent in red (after Galluccio and Scotti, 2022).

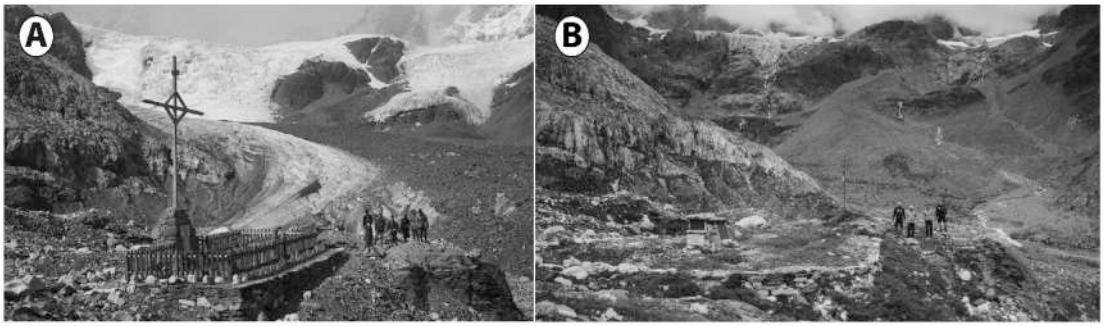

Fig. 3. (A) The "Cimitero degli Alpini" (Alpine cemetry) in the Vallone dello Scerscen in 1926, at the border of the tongue of the glacier with the same name (Photo by Alfredo Corti, © CAI Valtellinese) (B) The Vallone dello Scerscen. All what remains today of the ancient cemetry of the alpine soldiers swept away by an avalanche in 1917 is a gravestone and the supporting wall. The glacier tongue is reduced to some slender offshoots exiting from the upper ice mass (Photo taken in 2020 by Fabiano Ventura, © Associazione Macromicro).

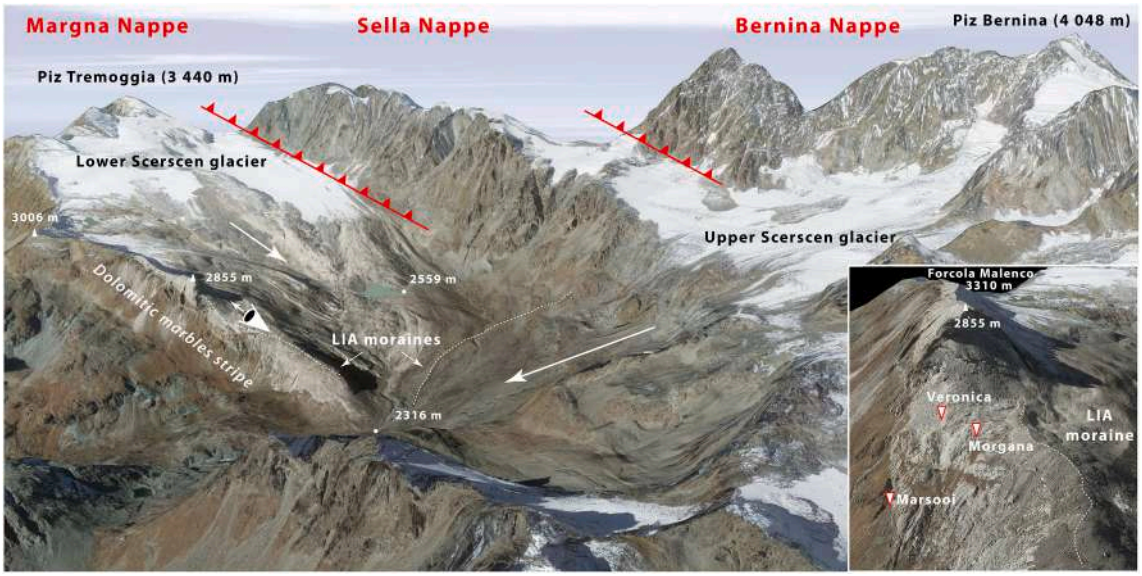

Fig. 4. Recent panoramic view of the Scerscen area. Caves open at the edge of the Little Ice Age (LIA) moraines between 2500 and 2600 m a.s.l. (view to the NW from Google Earth, the zoomed area (shown by the funnel on the Dolomitic marble stripe on the main panel) is viewed to the W).

(XRPD) and scanning electron microscope with EDS analyses (SEM-EDS) at the DISTAV laboratories (University of Genova). For further details on methods see Galliano et al. (2022).

3.2. *Cave mapping, geomorphological observations, sampling, and microclimate monitoring*

Three important caves were discovered, explored and mapped: Veronica, Marsooi and Morgana caves. The first cave surveys were carried out with traditional methods (compass, clinometer and measuring tape) in 1989 and 1990 (Veronica and Morgana caves, respectively). The caves were reexplored and surveyed using Disto-X (Heeb, 2014) in 2007 and in different years since 2017 (Fig. 7). The caves were visited several times between 2017 and 2023 to carry out geomorphological observations, sampling, installing and download monitoring instruments, and document speleogens and overall cave wall morphologies. Secondary minerals and rock samples of the different carbonate lithologies were taken both in surface outcrops and in the caves.

Monitoring of air relative humidity (RH) and temperature (T) was carried out only in Veronica cave, being the most easy-to-access cave (entrance does not close by snow each winter) (Fig. 8). Eleven dataloggers have been put in five different places inside the cave, and two dataloggers outside, close to the entrance. Six dataloggers where installed in July 2021 and controlled in September to check battery consumption, and other seven were put in place in October. All instruments remained for about two years in the cave until October 2023. All the five places in the cave were equipped with two dataloggers at different heights: one datalogger ca. 50–100 cm from the floor, the other at variable heights, from 3 to 4.95 m. The dataloggers used where eleven T-RH Elitech RC-51H, and two T Gemini Tinytag Plus 2 (point D - with 3 different probes: two at 30–300 cm from the floor respectively and one inside a fissure in the rock). In the range of the recorded T, the Elitech RC-51H resolution and accuracy are 0.1 and 0.5 °C, respectively. For RH comprised between 10 and 95 %, its resolution and accuracy are 0.1 and 3 %, respectively. Beyond 95 % RH, the accuracy is limited to 5 %. The Gemini Tinytag Plus 2 resolution and accuracy are 0.01 and around 0.5 °C, respectively. Unfortunately not all of them worked for the whole period, due to very cold conditions (low batteries) and to water condensation on instruments, which caused some misfunctioning.

3.3. *Water tracing test and chemistry*

A tracing test was carried out on July 2021 injecting 50 g of fluorescein ($C_{20}H_{12}O_5$, CAS number 2321-07-05) in the small underground river flowing in Morgana Cave, at −102 m depth from the entrance

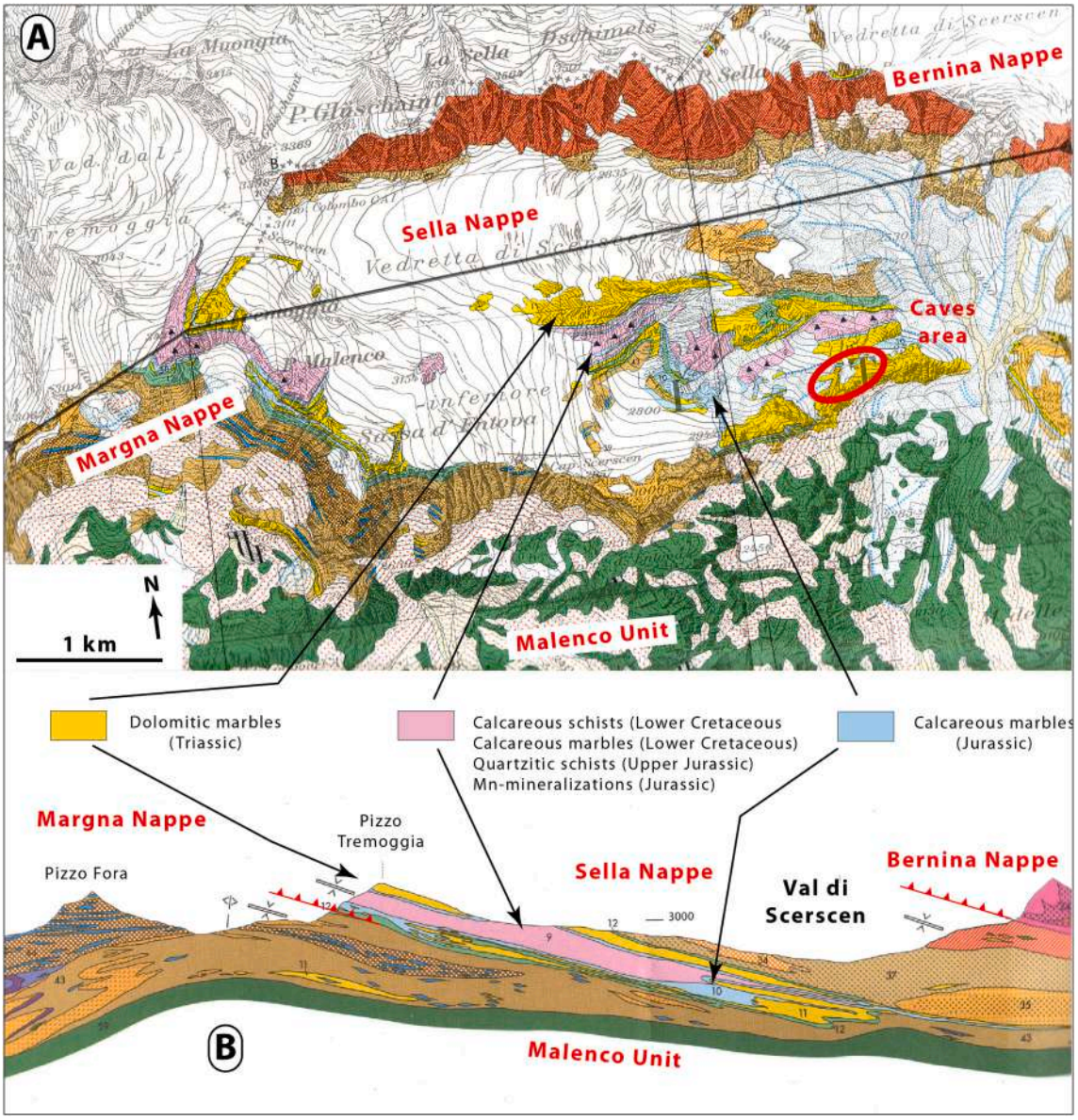

Fig. 5. Geology of the upper Scerscen Valley (after Montrasio et al., 2004). (A) Geological map. The glacier area is referred to 2004. (B) Geological profile with the overthrusting sheets and the recumbent syncline fold in the sedimentary cover. Profile location is indicated on map A.

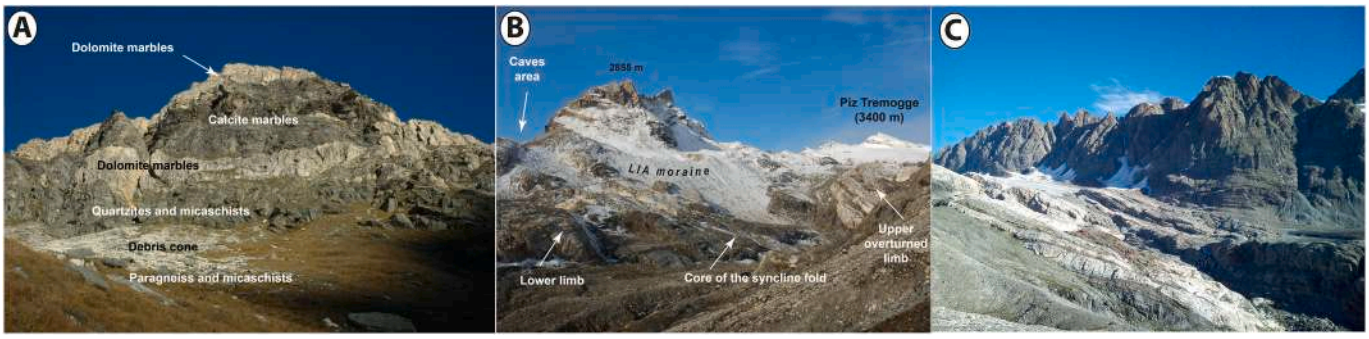

Fig. 6. (A) Picture of the marble outcrop where the caves are located: the caves are on top of the walls to the right (Photo Mauro Inglese). (B) In the upper portion of Scerscen Valley, the geological structure of the Margna nappe sedimentary cover is clearly visible, marked by the white beds of dolomitic marbles: to the west (left), the lower limb of the fold, to the east (right) the overturned upper limb, which can be followed to the very top of Piz Tremogge (Photo Andrea Maconi). (C) The recumbent syncline fold in the sedimentary cover of the Margna Nappe, with the white stripe of dolomitic marbles, overthrusted by the green-grey micaschists and the dark grey intrusive rocks of the Sella Nappe. In the upper left corner the retreating Lower Scerscen Glacier is still visible, once covering the whole Scerscen valley: due to glacier retreat, an increasing area of the sedimentary rocks is cropping out in the last decades (Photo by Mauro Inglese).

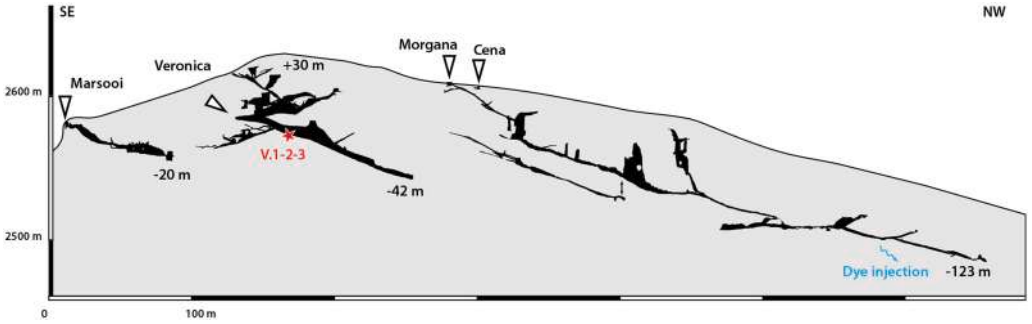

Fig. 7. Extended profile views of Veronica, Marsooi, Morgana, and Cena caves. Note that extended profiles of the caves do not perfectly respect their relative position and the distance to the surface. Sample locations of quartz pebbles (V1 to 3) and the dye injection point are indicated. Surveys by Gruppo Grotte Milano CAI-SEM.

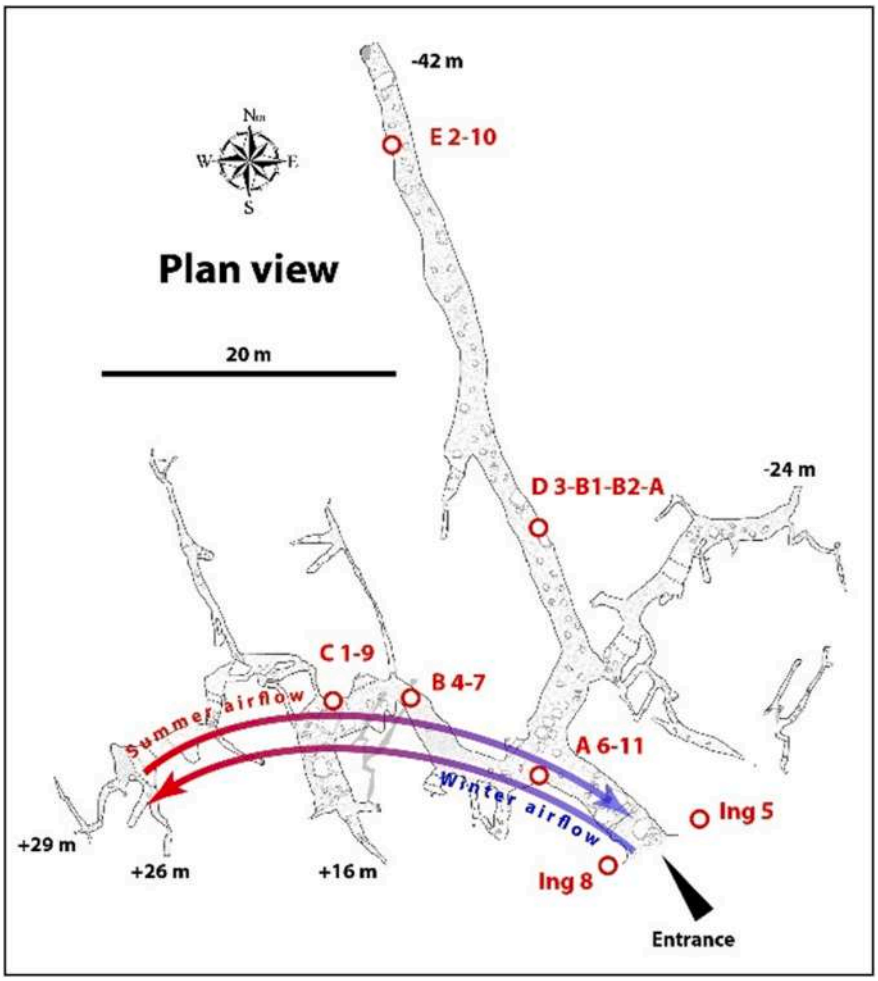

Fig. 8. Location of T and RH dataloggers in Veronica Cave (no. 1–11: Elitech; B1, B2 and A: Tinytag) and dominant seasonal airflow.

(location on Fig. 7). Morgana cave was chosen being the only one with permanent underground water flow. The flowrate was ca. 0.1 l/s and injection of the dye took approximately 10 min. Charcoal detectors were placed in four spots (Figs. 7, 8): a small surface stream (C1) that collects all the waters coming out from the carbonate stripe, ca. 500 m ESE of the injection point (2373 m a.s.l.); the Prediletta Springs (C2, the main outlet of the karst system), 50 m N from C1 (2368 m a.s.l.); the torrent (C3) exiting from the ancient bottom of the Scerscen lake, downstream of the carbonate stripe at ca. 850 m ESE of the injection point (2320 m a.s.l.); and the torrent (C4) coming out of the Scerscen glacier, ca. 1100 m E of Morgana Cave (2328 m a.s.l.). Electrical conductivity (EC) and temperature (T) were measured in situ, together with a flow rate estimation, each time the charcoal detectors were sampled and replaced.

Three charcoal detectors (numbered 0, 1, and 2) were put in place on July 23, 2021, the day before the tracer injection (24/07/2021). Detector number 0 was left in place over the entire period of monitoring. At each charcoal detector collection, one was taken (lowest number) and a new one (consecutive number) was put in place. Collections and replacements took place on July 25, August 8, and August 10, 2021 (1, 15, and 17 days after injection, respectively), during programmed fieldtrips in the area (we expected arrival times of 1–3 weeks). Rainfall during this time interval occurred on July 25 (light rain), August 4 (heavy rain), and August 8 (light rain).

Charcoal detectors were wrapped in aluminum foil, dried and kept in

complete darkness in the laboratory. The tracer was eluted by immersing 10 g of charcoal for 15 min in an alcoholic potash solution, filtering the obtained solution. The concentration of fluorescein in the eluate was determined using standardized benchmarks and methodologies. Assuming the adsorption of the tracer by charcoal was constant over time, the concentration value was divided by the immersion time of the charcoal bags in order to obtain comparable results. The values were also compared with the blank charcoal detectors, which were immersed for 24 h in the control points prior to injection.

Eight water samples were taken for geochemical analysis on October 2 in 2021, four in caves and the other four outside at springs or in surface waters located below the marble stripe (Table 1). All samples are representative of the waters flowing through the karst system, as shown by the dye tracing experiment. A 500-ml bottle was sampled for major ion content, a 100-ml bottle was acidified in situ with HNO_3 (65 %) for the analysis of metals. Sample temperature, pH and EC were measured in situ. In addition, 9 other springs located at the base of the carbonate outcrops and 1 surface watercourse were surveyed (Table 1). For the latter, measures were carried out for temperature (T), electric conductivity (EC), and discharge (Q), which was calculated using the salt (NaCl) dilution method.

Waters were analyzed at the laboratory of the Dipartimento di Ingegneria dell'Ambiente, del Territorio e delle Infrastrutture (DIATI), Polytechnic of Turin (Italy), using the methodology provided in De Waele et al. (2025).

3.4. Cosmogenic burial dating

The terrestrial cosmogenic nuclide burial dating method relies on the change in the initial $^{26}Al/^{10}Be$ ratio of surface quartz-rich rocks exposed to cosmic ray bombardment, after erosion and fluvial transport, and subterranean deposition (Granger and Muzikar, 2001). When quartz is buried at sufficient depth nuclide production ceases, and the $^{26}Al/^{10}Be$ sample ratio decreases due to differential decay of ^{26}Al (half-time of 0.705 Myr) (Norris et al., 1983) and ^{10}Be (half-time of 1.387 Myr) (Chmeleff et al., 2010; Korschinek et al., 2010). We sampled rounded quartz pebbles cemented to the floor in a lateral passage of Veronica Cave, around 40 m inside the cave. This area is overlain by ca. 50 m of marble rock above, so is perfectly shielded from incoming cosmic rays. This is what remains of a much larger deposit that probably filled the cave entirely, and appears to have entered from the surface by flowing water. We did not sample the smaller quartz pebbles profusely found in the actively drained passages in Morgana Cave: these conglomerates are composed of mm-to-cm-sized rounded quartz grains embedded in clayey cement, which are readily eroded by seasonal water flows, and are found all along the cave passage from 2570 m a.s.l. to around 2510 m a.s.l. Their "fresh" appearance ruled out the possibility to try a cosmogenic burial age calculation. Sample preparations were performed at LN2C (CEREGE, Aix en Provence) using the procedures described in Calvet et al. (2024).

Table 1
Water sample sites description. The first 4 rows (samples Ve and Mo) correspond to cave waters; the other rows are springs which were monitored during the dye tracing experiment.

Sample	Site	Description	Location of monitored springs (Lat.°, Long.°, alt. m)
Ve1	Veronica Cave	Final still-standing water pool	/
Mo1	Morgana Cave	Underground river at −80 m	/
Mo2	Morgana Cave	Waterfall branch at −50 m	/
Mo3	Morgana Cave	Branch of the dripping at −40 m	/
C1-P7bis	Spring	External water flow	46.340223, 9.881092, 2373 m
C2-P8	La Prediletta	Small karst spring	46.341430, 9.883063, 2368 m
C3-P10	External water flow	Seeping from a peatbog patch	46.339693, 9.889046, 2305 m
C4-P11	External water flow	Main Lanterna Torrent	46.342981, 9.891727, 2325 m
P1	Spring		46.339736, 9.869424, 2807 m
P2	Spring		46.339736, 9.869424, 2807 m
P3	Spring		46.338736, 9.876720, 2504 m
P4	Spring		46.339254, 9.879187, 2422 m
P5	Spring		46.339595, 9.878812, 2425 m
P6	Spring		46.340314, 9.879895, 2403 m
P9	Spring		46.341180, 9.884434, 2355 m
P12	Spring		46.345980, 9.884305, 2412 m
P13	Spring		46.346631, 9.877224, 2470 m

4. Results

4.1. Petrography of the host rock and mineralogy of secondary deposits

There are essentially two carbonate rock types in the cave area: a dark-grey to black calcite marble, and a whitish dolomite marble (Fig. 11). The first is characterized by a well-crystallized metamorphic rock composed of fine calcite crystals (ca. 0.1 mm in diameter) crossed with finer microcrystalline dolomite bands (crystals of 0.01 mm in diameter) containing minerals with high refractive indices (probably talc and tremolite) (Fig. 11A, B). This rock also contains some quartz grains and opaque minerals (pyrite and its oxidation products), and SEM-EDS confirmed pyrite and also some zircon crystals. The white metamorphic rock, on the other hand, is composed of very fine sub-euhedral dolomite crystals (diameter of a few microns), containing some veins of dolomite (with crystals of a few tens of microns) (Fig. 11C, D) with talc, tremolite, and pyrite inclusions, and minor amounts of zircon, rutile, quartz and barite, as confirmed by SEM-EDS.

Cave minerals were identified using XRD (Table 2). In Veronica Cave, the soft white deposits growing at the foot of the wall appear to be hydromagnesite. In Marsooi Cave, bushy popcorns are composed of calcite, with traces of vanadinite, whereas gypsum constituted the white crusts. Dolomite, instead, could be either part of the host rock or a secondary mineral. All of these minerals require extremely dry conditions to precipitate, which are seasonally present when evaporation occurs (Hill and Forti, 1997).

4.2. Geomorphology

Three main caves (Veronica, Morgana, and Marsooi), and one smaller one (Grotta della Cena, or Cave of the Dinner) were investigated in the area (Table 3, Figs. 7, 9, Supplementary Fig. 1). Veronica Cave opens at 2615 m a.s.l., and was the first to be discovered, with a length of 638 m in rising and descending branches. Tana dei Marsooi is a narrow

Table 2
Secondary cave minerals identified by XRD.

Sample	Cave	Characteristics	Minerals
VE1	Veronica	White deposits at the foot of the wall	Hydromagnesite
–	Marsooi	Popcorn	Calcite with vanadinite traces
tana1	Marsooi	Crust	Gypsum
tana2	Marsooi	Crust	Gypsum, dolomite

fissure opening at 2580 m a.s.l.. The largest and most complex is Morgana Cave, opening at 2610 m a.s.l., with a length of 905 m and a depth of 123 m. The smaller Grotta della Cena opens close to Morgana Cave at 2600 m a.s.l..

Veronica Cave has a 5-m wide and 2-m high entrance portal, equipped with a gate, giving access to three distinct cave branches. The dolomite marble in this entrance area shows some portions containing pyrite crystals and their corrosion aureoles (Fig. 12A). The entrance area exhibits frost-related rock shattering. The large Western branch (Fig. 12B) follows the main fracture sets (NNW-SSE and WSW-ENE) and ends in a few boulder chokes rising towards the surface, one of which showing a rising meander with a wavy and cupola-containing roof. The main passage descends in the NNW direction, and keeps the dimensions of the entrance part (ca. 4 m wide and 5 m high), showing a uniform slope of around 20°. It ends blind in a small water pool at a depth of 42 m below the entrance. This passage hosts many large meter-sized cupola, inclined along the available fractures, which often contain aligned smaller concave morphologies (solution pockets) (Fig. 12C). In several places along the walls there are also dark brown veins protruding several centimeters from the marble rock. These boxworks are mainly composed of Mn and Fe oxides, and their differential erosion has brought them into relief. In the upper walls and along the roof there are also "grooved" surfaces (Fig. 12F): minor fractures are dissolved preferentially. Slabs of rock, often rounded and smoothed by corrosion, are found on the ground. Detachment surfaces on ceilings are generally absent, erased by condensation-corrosion (Fig. 12B, D). White secondary deposits on the lower walls of the cave revealed to be hydromagnesite. The upper parts (walls and ceiling) of all main passages are often characterized by wavy morphologies (Fig. 12B, C, F), and in some areas by sloping facet-like (*Fazetten*) surfaces. There are no speleothems at all. The Eastern branch is characterized by a wide but low descending passage directed NE-SW. Here is found what remains of a larger fluvioglacial deposit containing quartz and metamorphic rounded pebbles (up to 4 cm in diameter) (Fig. 12E), partially cemented but later altered by condensation-corrosion dissolution. This is clearly an older deposit, different from the fine-grained fluvioglacial conglomerates (with centimetric pebbles) found especially in Morgana Cave, and was therefore sampled for cosmogenic burial dating. In general, however, Veronica Cave lacks important fluvial sediments (besides the just mentioned older ones).

Tana dei Marsooi Cave is a linear passage following a NNW-SSE and NW-SE fracture down to a depth of 20 m, where it ends on a narrow bedding plane and a vertical fissure. The ceiling is carved with a wavy ceiling channel, whereas the lower and middle walls are covered with calcite and aragonite popcorns (Fig. 13A). In some places gypsum has also been found (Fig. 13B).

Morgana Cave, at a first glance, is very different from both Veronica and Tana dei Marsooi. It has a rather narrow entrance at the bottom of a small collapse, giving access to a steeply inclined (30°) elliptical tube 2 m wide and 1.5 m high descending eastward. This passage leads twenty meters further down to a 15 m-deep shaft whose bottom is littered with big marble blocks. Here, the main water flow derives from a narrow passage located south (Branch of the dripping), running down into a regular 20° dipping canyon, 2 m wide and several meters high, with a shallow (a few decimeters deep) vadose incision (Fig. 13C). This passage is clearly fracture-guided and descends for 70 m in a NNW-SSE direction. Here a narrow ascending branch (Waterfall branch) develops a little over 100 m in the southern direction, eventually arriving near the surface. Continuing the main branch northwards, the passage becomes less inclined first (the running water forming some small pools) before resuming the NNE direction and returning to be steeper (20°). Fifty meters further down the conduit ends in a vertical shaft leading into a vertical *E*-W fissure with a horizontal sediment-covered floor. The walls of this vertical canyon-like passage are covered with remains of a fluvioglacial conglomerate, with well-sorted pebbles of a few millimeters to a centimeter in size, which appears to have filled the entire passage up to several meters height (Fig. 13D). These pebbles are loosely held together in the fine-grained sediments characterizing the floor. In this fissure, at 102 m of depth, the small stream disappears into an inaccessible hole in this area of the cave; this is where the dye tracer was diluted. A 20-m long crawlway eastward leads into a cylindrical conduit of 2.5 m diameter, which descends with a slope of ca. 20° over a distance of 100 m towards the north before ending in a sediment choke. The walls are coated here with a thin veneer of still liquid mud. As for Morgana Cave, there are no speleothems at all, whereas the dark-blackish boxworks are seen in several places.

Below the access to Morgana Cave there is another entrance leading into a 10-m long elliptical conduit opening on the vertical wall. This smaller cave is called Grotta della Cena (Cave of the Dinner), since it is one of the most comfortable sites to shelter during windy and rainy/snowy weather. This is clearly a part of Morgana Cave, separated from it by a small collapse doline. The Grotta della Cena appears to be an old phreatic tube, from which Morgana Cave would be a younger undercut. The elliptical tube follows the foliation plane, and its floor is characterized by a 45° sloping wall (facet) which appears to have retreated by ca. 10–15 cm due to corrosion (snowmelt and/or condensation waters).

4.3. Water chemistry and dye tracing

The caves opening up on the top of the marble stripe contain seasonal flowing water, which drains down and exits at the foot of the almost vertical cliffs, near the contact with the adjacent schists, or from the debris cone deposits located around 100 m below the caves (Figs. 9, 10). Chemical analysis shows typical values of waters in contact with carbonate rocks (Table 4). The Veronica sample (Ve1) has much lower values in Ca and Mg, probably related to the input of less mineralized snowmelt and condensation waters. In Morgana water samples, sulfate contents are one magnitude greater than in Veronica cave, which is likely related to the oxidation of sulfides in the host rock. The external (spring) samples generally have lower mineralization, although still containing the typical Ca-Mg-carbonate fingerprint, and are probably in part diluted by snowmelt water. For other surveyed springs, 2 different groups of waters are recognized (Table 4): "karst" and "slope" waters. Karst waters, C2-P8 and P13, are characterized by relatively high mineralization (EC around 200 μS/cm) and low temperature (2.2 to 3.7 °C), consistent with the characteristics of a karstified aquifer. Spring waters coming out of slope debris have a mineralization dependent on the prevailing lithological nature of the clasts: lower where phyllites prevail (75–150 μS/cm), higher where carbonates prevail. T are generally higher due to the superficial character of the aquifer and water flow: measurements were made in a summer context, which favors warming of the water by solar energy.

The hydrogeological setting of the area consists of a carbonate complex, mainly marbles (Figs. 5, 6). These are interspersed between

Table 3
Location, speleometric data, and exploration of the studied caves.

Cave	Lat. (°N), Long. (°E)	Alt. (m)	Speleological register no.	Depth (m)	Length (m)	Discoverers (date)
Veronica Cave	46.3413733, 9.8767247	2615	Lo/So 3088	71 (−42/+29)	638	Giovanni Bardea (1986)
Tana dei Marsooi	46.3406984, 9.8767139	2580	Lo/So 3093	−20	77	Mario and Renzo Salvetti (1986)
Morgana Cave	46.3419957, 9.8777092	2610	Lo/So 3087	−123	905	Gruppo Grotte Milano CAI-SEM (1990)
Grotta della Cena	46.3419504, 9.8777475	2600	Lo/So 3123	−2	10	

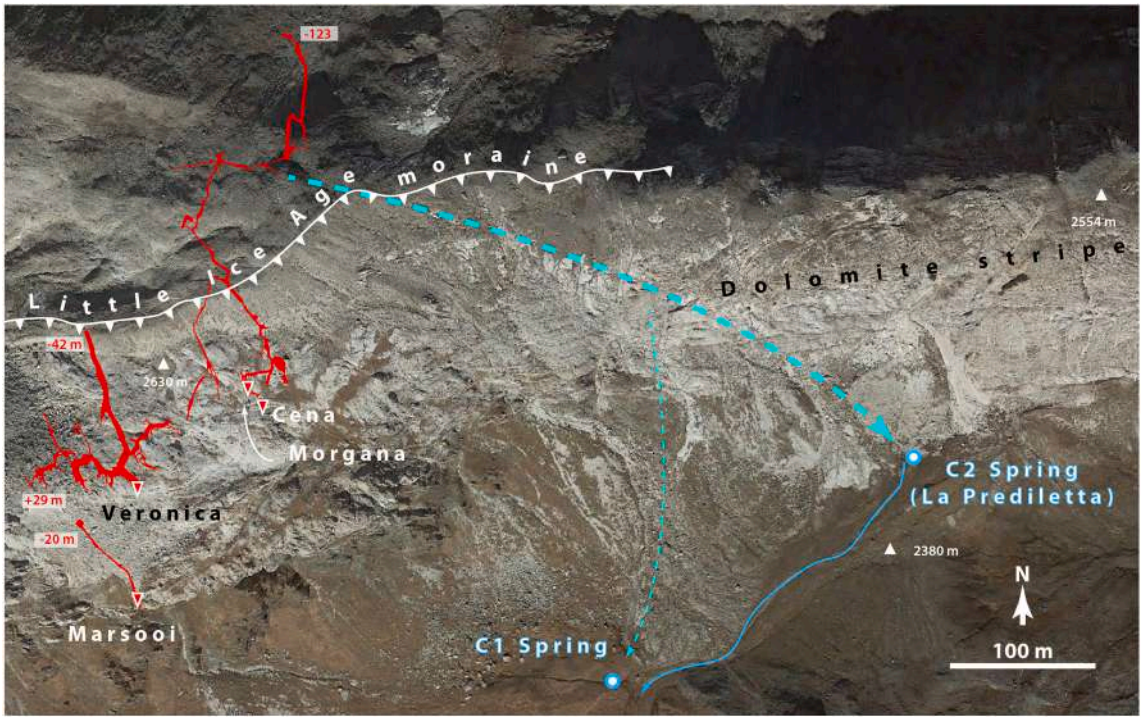

Fig. 9. Map of caves, injection point, water sampling points, and monitored springs during the dye tracing test. The *E*-W dolomite stripe outcrop appears in light colour across the center of the image. The light blue arrows show the hydrological connection. For position of C3 and C4 (out of this figure to the right) see Fig. 10.

Fig. 10. Positions of the springs surveyed with charcoal detectors: caves are on the left, on top of the ridge (Photo Mauro Inglese).

crystalline metamorphic units characterized by low primary and secondary permeability. The lithologic sequence is covered, also extensively, by slope debris, with high primary permeability, glacial deposits, with variable, but overall low permeability, and lacustrine sediments, associated with the dam determined by a large landslide. Alluvial sediments, with high permeability, are present along stream beds, generating local elongated aquifers of modest extension. The main hydrogeological objectives were: i) recognizing the role of surface deposits and distinguishing springs fed by the carbonate complex from others, and ii) characterizing the carbonate aquifer, especially its degree of karstification. To verify the degree of karstification of the carbonate aquifer and the dynamics of its waters, a dye tracing test was carried out in the summer period, characterized by alternating sunny periods and precipitation, some intense, even snowfall at the highest elevations.

The dye tracing test showed that spring C2 ("La Prediletta") was found to be positive, with arrival of tracer in high concentrations within 24 h (or less) after the injection (Fig. 14). The second observed peak corresponds to the rainfall that occurred between August 9 and 11,

Table 4
Water sample analysis (all values in mg/L). Physical measurements (EC and T) were made in summer 2021 (July 23 / Aug. 10). Ve corresponds to Veronica drippings; Mo to Morgana Cave flows; C1–4 to the springs monitored during the tracing experiment.

Sample	Ca^{2+}	Mg^{2+}	Na^{+}	K^{+}	Cl^{-}	SO_4^{2-}	HCO_3^{+}	NO_3^{-}	EC (µS/cm)	T (°C)	Q (l/s)
Ve1	16.1	8.1	0.10	0.12	0.13	7.51	77.56	2.6			
Mo1	33.4	16.3	0.15	0.37	0.07	92.44	65.66	1.3	370	1.9	
Mo2	32.5	18.4	0.19	0.32	0.10	89.94	76.18	1.4	311	2.0	
Mo3	29.1	17.1	0.19	0.36	0.09	70.35	85.29	1.0	245	2.1	
C1-P7bis	28.1	9.9	0.26	0.35	0.06	10.63	122.69	0.3	191.4 / 188.0	10.2 / 8.6	10.0
C2-P8	21.8	9.4	0.27	0.30	0.13	24.92	82.53	0.7	193.4 / 174.0	2.2 / 3.2	10.0
C3-P10	34.2	12.2	0.35	0.95	0.08	11.10	153.87	0.0	311	22.7	5.0
C4-P11	18.5	3.9	0.51	0.55	0.10	44.38	20.29	0.5	73.4	8.5	≈3000
P1									79.5	11.3	0.5
P2									117.2	5.3	2.0
P3									148	6.7	0.2
P4									144.5	8.8	8.0
P5									224.6	7.0	2.0
P6									225	4.8	2.0
P9									201	7.3	0.1
P12									285	11.0	0.1
P13									184	3.7	0.2

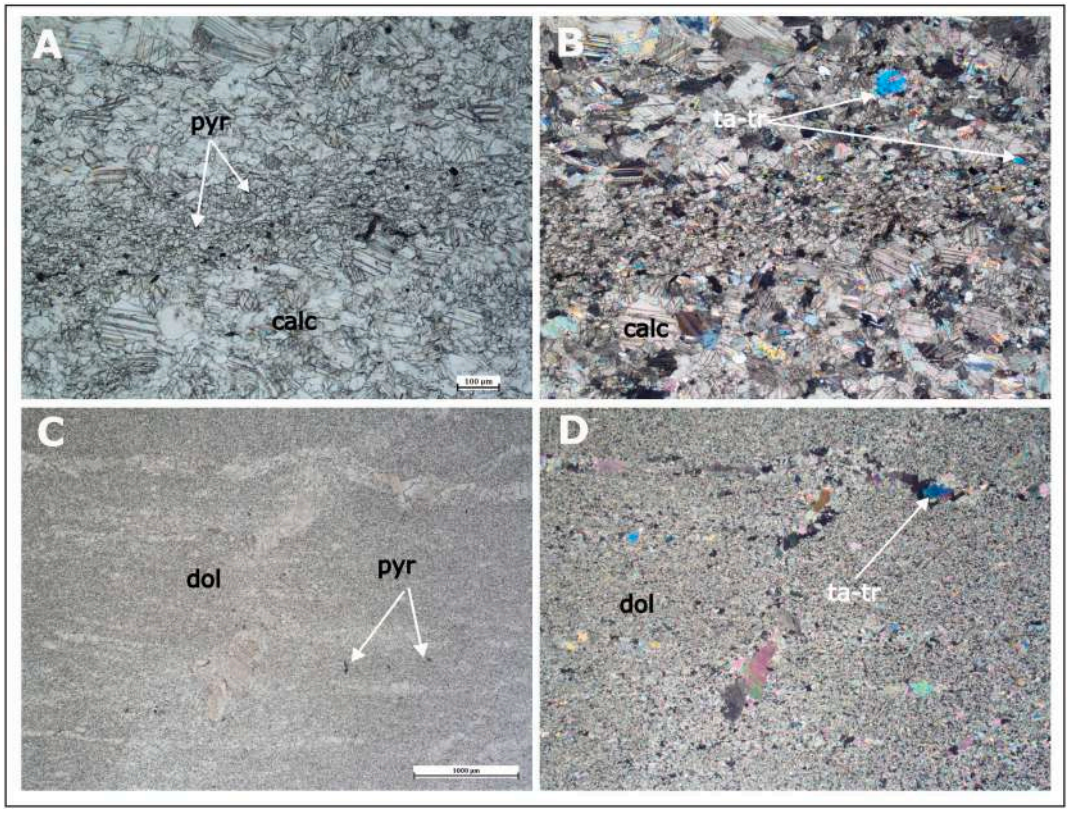

Fig. 11. Thin section of the dark grey calcite marble (A–B) and the whitish dolomite marble (C–D). Parallel (A–C) and crossed nicols (B–D) (Note scale is the same). A fine-grained calcite (calc) layer is visible in the calcite marble, containing opaque minerals (black crystals in A, mainly pyrite, pyr) and minerals with third-order colour in B (probably talc or tremolite, ta-tr). The finer-grained dolomite (dol) marble contains veins of larger crystals also with tiny opaque crystals (C, pyrite) and minerals with third-order colors (D, mainly talc and tremolite).

2021. The control point C1, located further downstream and fed by several small springs at the base of the carbonate wall, was affected by a slower restitution, while the highest control points, i.e., slope springs C3 and C4, remained negative. The peak velocity values were calculated on the basis of the analytical outcomes (Table 5, Fig. 14).

4.4. Cosmogenic burial dating

Three different samples (located on Figs. 7, 8) were analyzed, but only one of these delivered a reliable burial age (V1) (Table 6). V2 and V3 gave blanks (i.e., measured Al and Be ratios were too low, so it was possible only to estimate a minimum age), and burial age was estimated using the highest measured concentrations, which have to be considered minimum ages. Although V3 has given a similar age as V1, the first is a minimum age, whereas the second is a reliable one. V2, on the other hand, delivered a much younger age (note this too is a minimum age), and might reflect a more recent entrance of these pebbles into the cave. In conclusion, anyhow, the age reflects a burial of fluvioglacial pebbles into Veronica Cave at least around 1.3 ± 0.4 Ma.

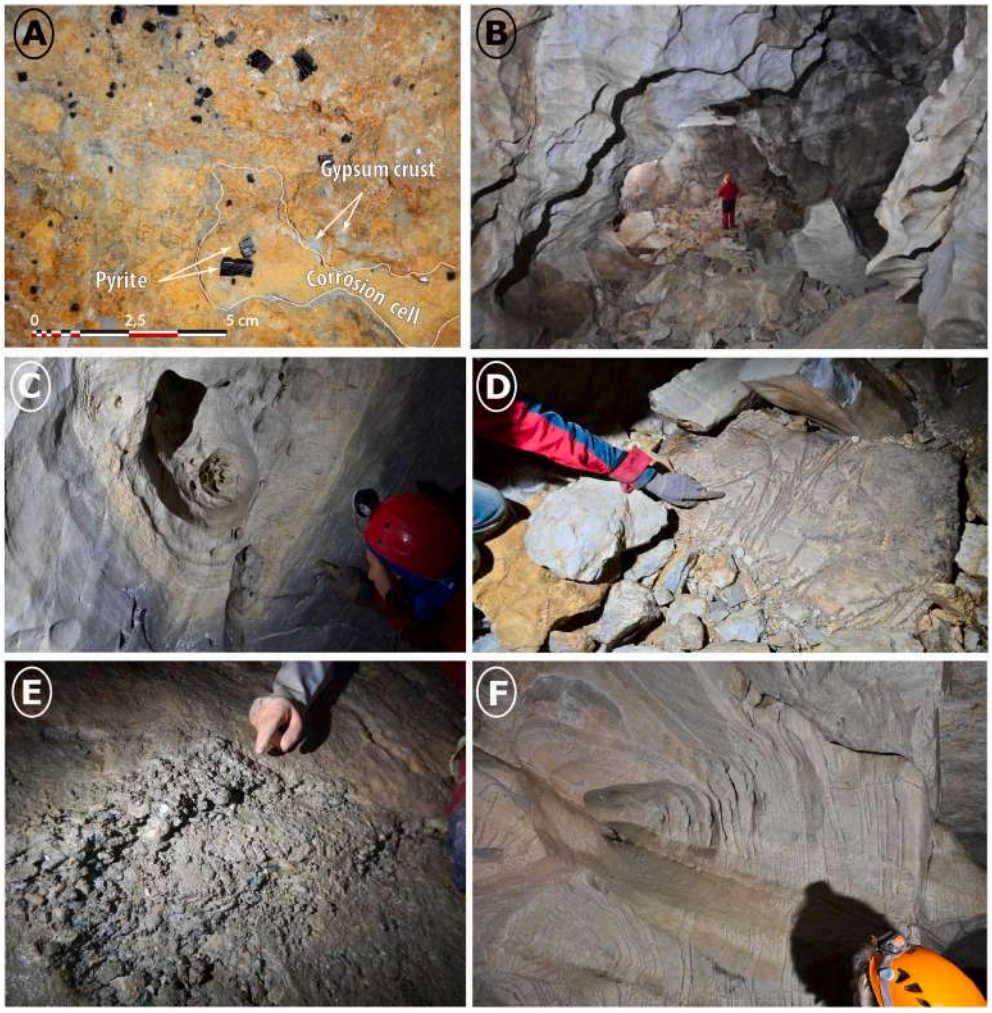

Fig. 12. Veronica Cave. (A) Millimetric pyrite crystals in the dolomite marbles close to the entrance of the cave (Photo Didier Cailhol). (B) Large old phreatic passage with important breakdown deposits on the floor in the western branch (Photo by Mauro Inglese). (C) Cupolas with nested solution pockets. Note the wavy walls (Photos by Mauro Inglese). (D) The floor covered with angular marble slabs and blocks: note the grooved rock surface (Photo by Mauro Inglese). (E) The fluvioglacial deposit with centimetric quartz and schist pebbles (Photo by Didier Cailhol). (F) The enlarged grooves following the foliation planes. Note they develop along the wavy marble wall of the cave (Photo by Mauro Inglese). For location of pictures see Supplementary Fig. 1.

4.5. Cave microclimate

Preliminary results enable us to better characterize temperature and humidity conditions in Veronica Cave. During summer (when the cave can be visited) warmer airflow enters from the western (upper) branch and flows down to the entrance while cooling (Fig. 8), but also creates some convectional cells in the initial parts of the descending galleries. During winter, the cave entrance is often blocked by snow, limiting airflow, but when it reopens cold air rises up into the passages causing dry evaporative conditions in the whole cave (Figs. 8, 15, 16). On average, temperatures remain rather cold: +1.60 °C in average. The warming periods starts in March–April, with a gradual T increase of the baseline from +2 to +3.5 °C, with numerous short peaks at +4 up to +5.7 °C at the maximum. The cooling period starts at different times, in October for 2021 but as soon as August for 2022, as shown by T decreases (reaching −1 to −6 °C). When snow covers the entrance, it blocks air exchange with the surface. In 2021, it occurred late in winter (January 2022), but much earlier the next year (mid-August 2022). Inner T then stabilizes around +1.5 to +2 °C, and regularly decreases slowly by about 0.05 °C/month, as a result of the cold wave penetration inside the rock. Since the snow cover is blown and accumulated by wind at the entrance, it is generally long-lasting till July, but air begins circulating again early, in February or March.

The standard deviation analysis of temperature along the main gallery (points A-D-E), shows a strong attenuation of seasonal variations related to distance from entrance (Fig. 16): this is not surprising, and highlights that energy exchanges with the surface are limited to the first reach of the cave. In addition, dataloggers close to the roof have a larger distance of surface influence than dataloggers placed at the floors: this can indicate a greater influence of summer airflow on cave temperatures that cools down during its descending through the cave and leads to condensation-corrosion processes.

These entrance parts are clearly exposed to condensation phenomena, with droplets seen on the cooler upper cave walls and ceiling. The RH record shows that humidity is at saturation, both during the warming period when “hot” external air cools down while entering, and when the cave becomes isolated under the snow cover (Fig. 15). On the contrary, during the cooling period (mainly autumn or during some short summer events), the introduction of cold air from outside that warms up in the cave lowers RH, with peaks below 70 to 50 %, at the origin of strong evaporation conditions.

Tana dei Marsooi was not monitored, however observations showed that during summer, the air in the cave is cold and stable: it acts as a cold trap. During winter, warm air rises from the lowest point in the cave, leading to condensation in the upper parts, and is replaced by cold air sucked in from the outside, leading to evaporative conditions in the

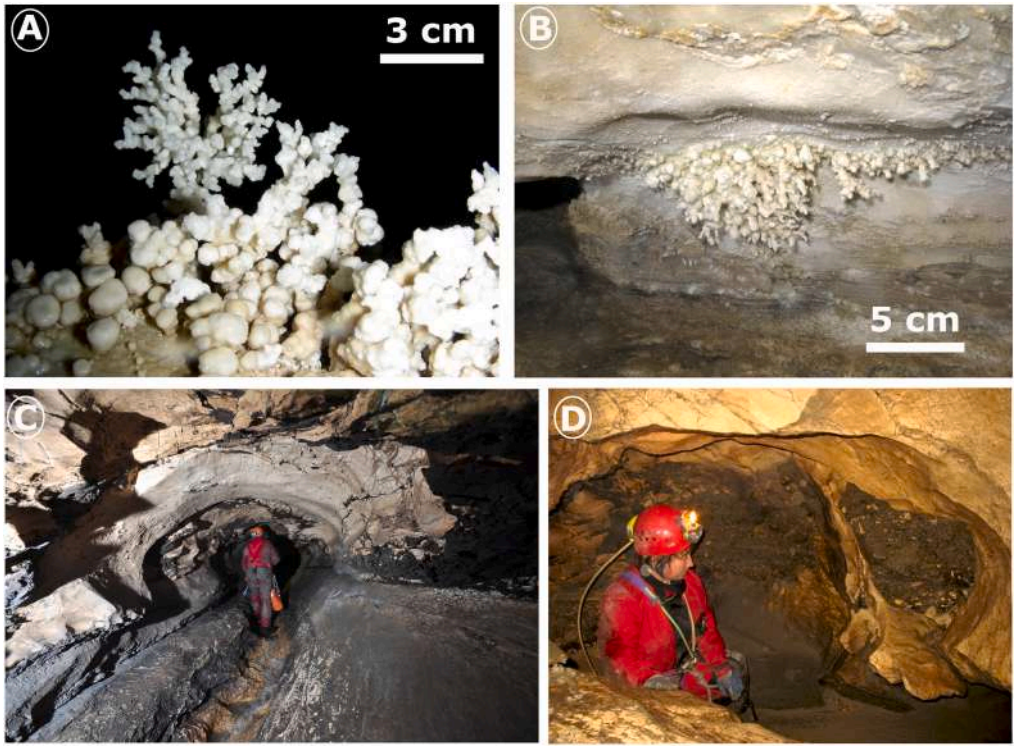

Fig. 13. Marsooi Cave. (A) Calcite-aragonite popcorn (Photo by Ivano Foianini). (B) Gypsum crusts (above) and aragonite bushes (center) (Photo by Mauro Inglese); Morgana Cave. (C) The elliptical descending conduit starting from the base of the shafts: note the blackish clay coating due to backflooding, and the shallow vadose incision with running water on the floor (Photo by Mauro Inglese). (D) The dark patches of fluvioglacial sediments, with pebbles held together by rather loose dark clay-sandy material, which almost entirely filled the conduit (Photo by Mauro Inglese). For location of pictures see Supplementary Fig. 1.

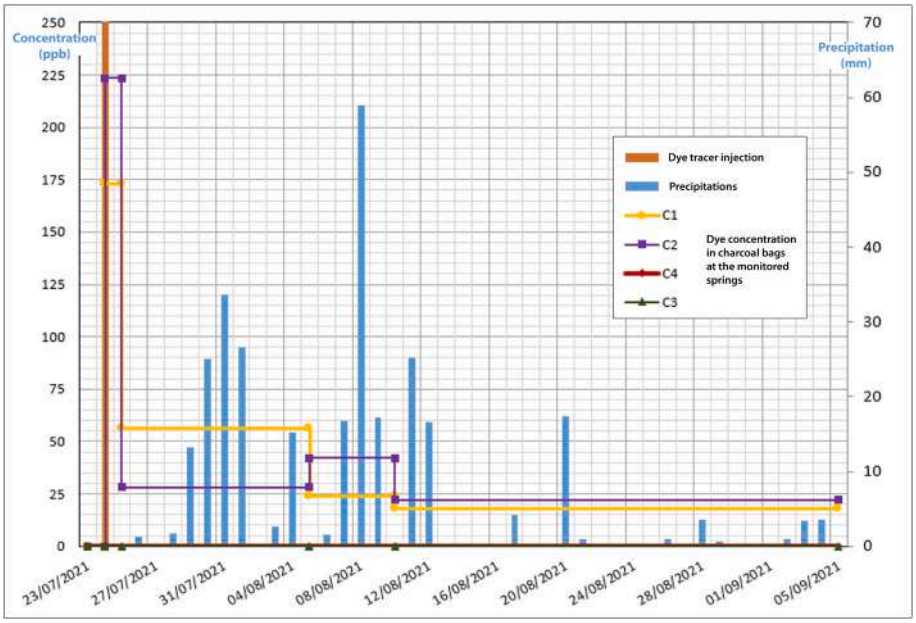

Fig. 14. Calculated concentration of fluoresceine in successive charcoal bags. Rainfall is indicated. C3 and C4 values are at 0.

lower parts of the cave passage.

5. Discussion

5.1. Pre-glacial cave development

Several studies have focused on ice-contact karst and speleogenesis, especially in Northern Europe (Lauritzen, 1986; Skoglund and Lauritzen, 2010; Skoglund et al., 2010), but also in the Alps (Audra, 2004; Spötl and Mangini, 2010). Earlier studies believed subglacial caves could form by waters circulating at the bottom of glaciers (e.g., Horn, 1935, 1978). Other authors (e.g., Corbel, 1957) believed caves mainly formed in proglacial conditions, due to the low temperature of the low-mineralized waters that enables CO_2 to dissolve with more ease. The

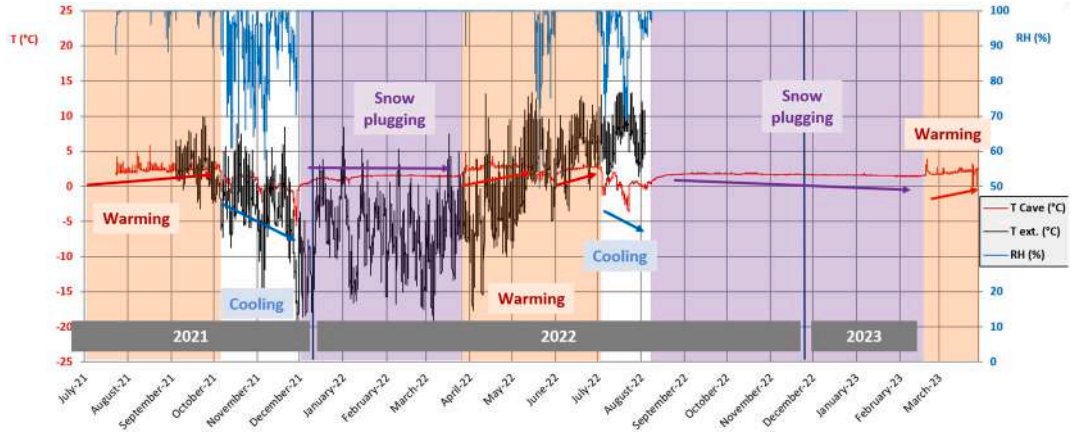

Fig. 15. Temperature and relative humidity measured over a period of two years in the entrance hall of Veronica Cave (point A located on Fig. 8). The black graph shows the external temperature measured at the ARPA surface meteo station of Rifugio Marinelli (3035 m a.s.l.), on the other side of the Scerscen valley (see location on Fig. 2).

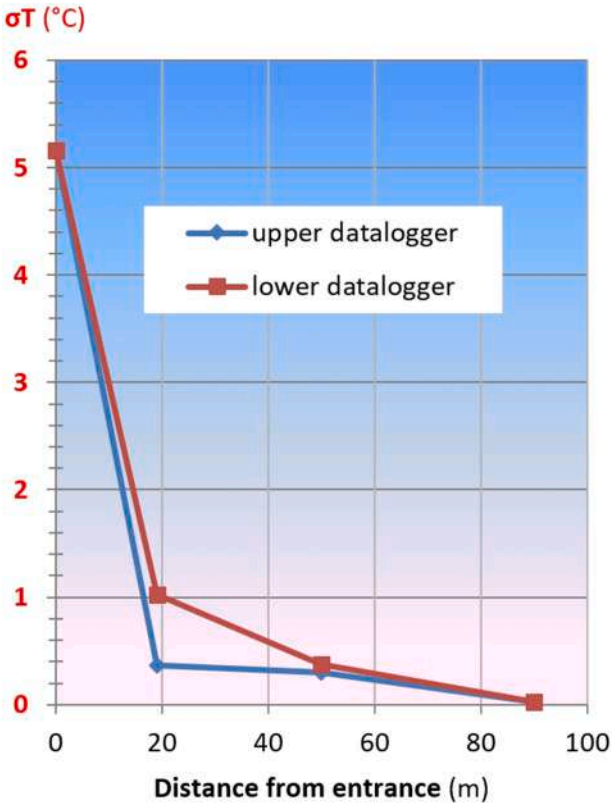

Fig. 16. Temperature standard deviation related to distance from entrance. Amplitude is greater close to the entrance, and rapidly attenuates with distance from entrance. Variations are sensible over a longer distance for the upper datalogger, high on the ceiling. At a distance of around 50 m, temperatures change very little over time.

problem is that CO_2 is low in meltwaters, especially when they are not in contact with the surface atmosphere, as often occurs below glaciers (subglacial conditions) (Lauritzen, 1986). Lack of soil and vegetation also does not provide extra CO_2, an essential player in the karst process, thus causing very languishing dissolution conditions. Moreover, if glacial meltwaters contain rock flour of carbonate composition, most of the poor aggressivity is soon exhausted, leaving little space for extra dissolution in fractures and conduits (Lauritzen and Skoglund, 2013).

Since the advent of U/Th dating methods, many studies have shown most ice-contact caves to be much older than the last ice ages (Lauritzen and Gascoyne, 1980; Audra, 2004). Studies in Spannagel Cave, a large cave system (11 km) located at around 2500 m a.s.l., close to the Hinterflux glacier in Austria, has shown the cave to have survived erosion over at least three glacial cycles, as demonstrated by U/Th dating of old speleothems (Spötl and Mangini, 2010). Even older caves have been found at high altitudes, demonstrating that in certain places very ancient caves can be preserved from glacial erosion even over millions of years (Audra et al., 2006). For example, Raponzolo Cave, in the Brenta Dolomites (Northern Italy) and located at 2560 m a.s.l., appears to be older than 5.25 Ma, according to burial ages of quartz sands found inside (Sauro et al., 2021).

True caves formed by the ice-contact meltwaters are rare: a good example is given by Kvithola in Northern Norway (Lauritzen, 1986). The cave formed along wall-parallel exfoliation planes in the Cambrian marbles, by meltwaters in contact with the atmosphere. This cave, whose age is not constrained, based on modelling might have formed in some ten thousands of years, and is probably of Late Last Glacial Maximum (LGM) age.

The presence of well-developed cave systems presently at 2600 m a.s.l, close to the retreating Scerscen Glacier, has raised some questions on how these caves formed, and what their relation was to the nearby glacial masses. The only reliable cosmogenic burial dating of Veronica Cave sediments has revealed an age of 1.3 ± 0.4 Ma, pointing to a rather old age at least of this cave. Morgana and Marsooi caves, on the contrary, have much smaller sizes (phreatic conduits are around 1/3 of the size of similar conduits found in Veronica Cave), and given their vicinity, this might simply be explained by their different age, the smaller caves being possibly much younger than Veronica. If Veronica Cave has formed prior to 1.3 ± 0.4 Ma, we have to consider it formed in a period in which its location was much lower than today. Although present-day uplift rates are around 1–2 m/ka, over the last 1 Ma average uplift rates should have been lower, and we can approximate a value of 1 m/ka (Sternai et al., 2019). Using this hypothetical value, and the minimal age of the cave (based on the only reliable burial age of 1.3 ± 0.4 Ma), the cave might have formed at an altitude around 1300 ± 200 m lower than where it is today, thus at ca. 1300 ± 200 m a.s.l. Of course, being only a minimal age, Veronica Cave might also be older, so it might have formed even at lower altitudes.

During the LGM, the Equilibrium Line Altitude (ELA) in the study area, now retreated at around 3000 m a.s.l., was at around 1500 ± 200 m a.s.l. (Višnjević et al., 2020), and this ELA must have been rather similar also during other important past glacial era (e.g., MIS6, MIS10, MIS12, MIS16). As an approximation, during MIS16 (676–621 ka ago) the caves would have been at approximately 1900 ± 200 m a.s.l., thus

Fig. 17. (A) Seepage gaining its aggressivity by the weathering of pyrite-rich allogenic sediments, close to Morgana Cave bottom. (B) Corroded boxwork with a thin veneer of calcite, Veronica Cave (photos Didier Cailhol).

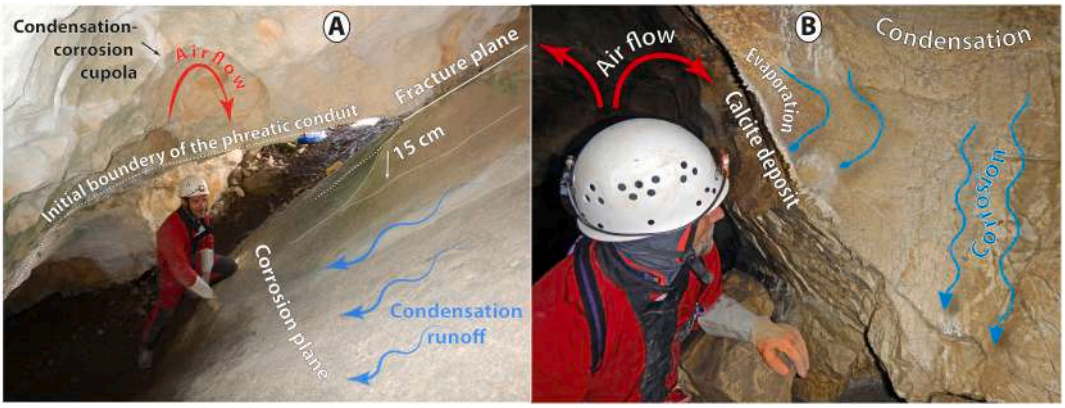

Fig. 18. Corrosion planes ("Facets") of condensation-corrosion. (A) "Grotta della Cena", the planar wall has retreated for about 15 cm. (B) Morgana Cave, local convection making both condensation and evaporation, resulting in calcite deposition and in planar facets (photos Didier Cailhol).

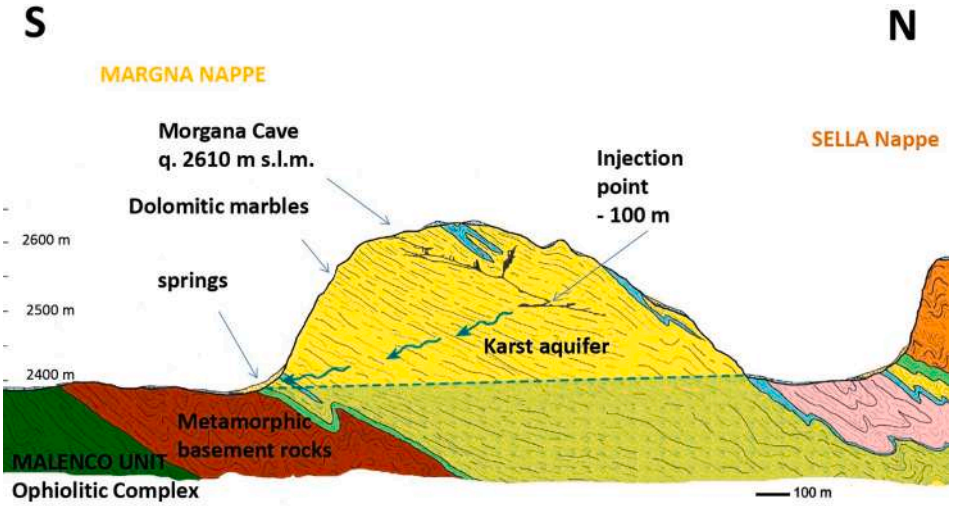

Fig. 19. Schematic section (not in scale) of the geological setting with cave survey, injection point and springs where the dye was recovered.

also well above the hypothetical ELA. The caves were thus presumably ice-covered, at least for part of their existence, and often (during glacial retreats and advancements) were located close to or at the ice margins. Also during the LGM, the cave was surely covered with ice over a certain period of time (being at around 2500 m a.s.l.). Although these are rough calculations, we have all confidence that the caves, now at 2600 m a.s.l., have been above the ELA during most of the maximum extensions of glaciers during the Middle to Late Pleistocene, and became thus marginal to the glaciers several times during warmer glacial retreat periods.

The minimal age of the cave (note Veronica Cave might be much

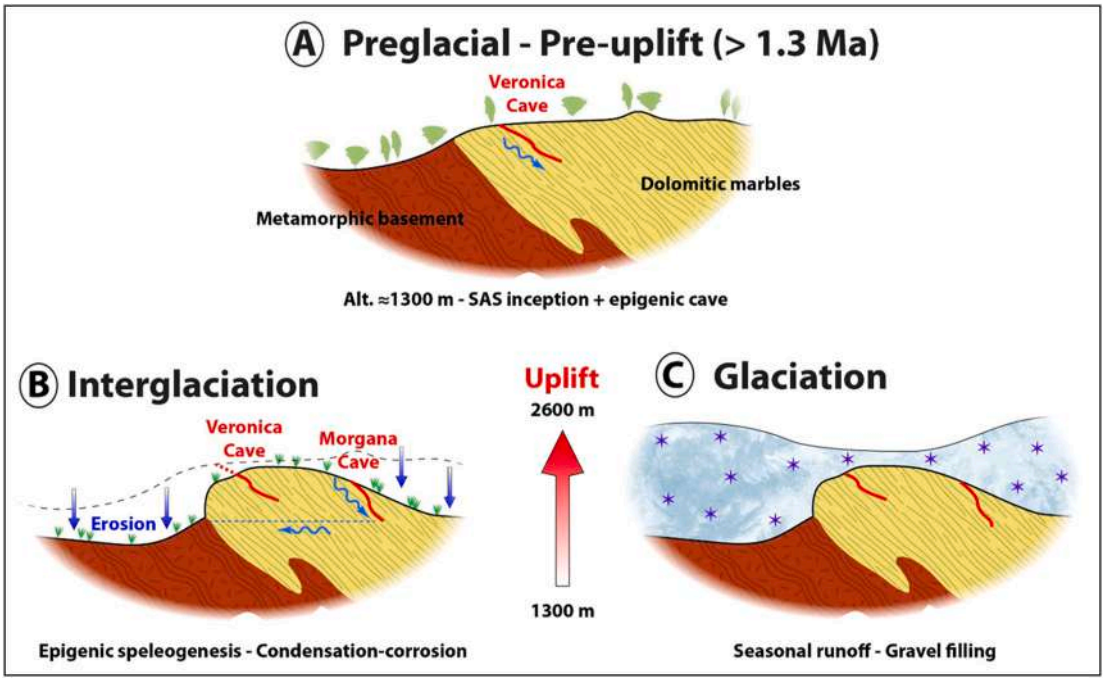

Fig. 20. Evolution of the Scerscen caves and karst according to alpine uplift and Pleistocene climates.

Table 5
Dye tracing results.

Sample	Site	Description	Dye recovering	Peak concentration (ppb)	Time to peak (h)	Distance (m)	Altitude Difference with injection point at 2508 m (m)	Apparent velocity (m/h)
C1	External water flow	Downstream reach of torrent	Positive	170	≈24	500	132	>21
C2	La Prediletta	Small karst spring	Positive	220	≈24	450	127	>19
C3	External water flow	Seeping from a peatbog patch	Negative	–	–	900	≈200	–
C4	External water flow	Downstream in Scerscen valley	Negative	–	–	1060	≈180	–

Table 6
^{10}Be and ^{26}Al concentrations and burial ages, obtained for samples taken in Veronica cave at 2590 m a.s.l. Detailed geochemistry data are provided in Suppl. Fig. 2.

Sample	^{10}Be (at/g)	^{26}Al (at/g)	^{26}Al/^{10}Be	Burial age (Ma)	Comments
V1	10.655 ± 1.561	38.687 ± 10.310	3.6308 ± 1.1041	1.293 ± 0.395	Reliable age
V2	1.118	5.953 ± N.D.	5.3262 ± N.D.	0.448 ± N.D.	Minimum age
V3	2.873	9.118 ± N.D.	3.1743 ± N.D.	1.545 ± N.D.	Minimum age

older) curiously corresponds to the onset of the switch from short- (41,000 years) to long-duration (100,000 year) glacial-interglacial cycles, characteristic of the Middle Pleistocene Transition (MPT). From 1.25 Ma up to around 700 ka, glaciers started to increase in thickness, volume, and duration, becoming more erosive in glacial valleys while preserving their high-mountain recharge areas from extensive erosion, the glaciers being less mobile here (Valla et al., 2011). In such situation, the marble stripes often remained in relief, surrounded by less resistant metamorphic shales, similar to situations known in Norway or Austria (Lauritzen, 2001; Audra, 2004). The so-called "major" glaciations appear to have started at around 0.9 Ma in the Western Alps (Muttoni et al., 2003). The burial date (although based on only one reliable burial age) suggest Veronica Cave to have been there before, formed at a middle mountain altitude (presumably at about 1300 ± 200 m a.s.l. or lower). This was thus probably well below the tree line, so there was plenty of CO_2 available especially during warmer Pleistocene periods. On average, each interglacial lasted for about 15,000 years (whereas glacials often lasted ca. 100,000 years). With around 17 interglacial periods since 1.3 Ma (starting with Marine Isotope Stage 37), this would lead to around 250 kyr of warmer intervals, a reasonable time period to carve cave systems as the ones we see today in Scerscen. Furthermore, the position of the fluvial deposit, very close to the entrance and with a surface topography which presently cannot supply any stream entering the cave, suggests the cave formed in a rather different topographic situation.

Another possibility is that the quartz pebbles were buried and transported under the glacier before entering the caves. If the ice was >100 m thick, the shielding against cosmogenic rays would have been sufficient. In that case the introduction of pebbles into the cave could be more recent. It is however difficult to state that pebbles under the glacier would always have been shielded by ice, especially during interglacials, when ice thickness and expansion reduced drastically. We therefore think this possibility can be discarded.

5.2. Sulfuric acid speleogenesis (SAS) from pyrite oxidation

SAS can be produced by deep-seated H_2S upwelling (De Waele et al., 2024), or by in situ oxidation of sulfides contained in the host rock (Auler and Smart, 2003; Audra et al., 2015; Webb, 2021). The local Mesozoic marbles contain pyrites, whose oxidation produces sulfuric acid, which reacts with the carbonates from the host rock to form sulfated by-products. The humidity required for oxidation is provided by summer air intakes cooling down in the cave and generating condensation, with the sulfates then being leached out by runoff. When conditions reverse in winter, with drying caused by air currents heating up as they enter the cave, evaporation leads to sulfate precipitation in the form of gypsum crusts [$CaSO_4{\cdot}2H_2O$] (Fig. 13B), as well as hydromagnesite deposits [$Mg_5(CO_3)_4(OH)_2{\cdot}4H_2O$]. In this carbonate mineral, Mg is derived from dissolution of the dolomitic host rock. The quantity of condensation waters is always rather low, so that dilution is prevented and acidity can be maintained over longer times, at least close to the sulfide oxidation points.

Grooved walls result from the condensation-corrosion that reveals the schistosity of the marbles (Fig. 12D, F). The only source of acidity responsible for this powerful corrosion is probably the oxidation of pyrites from the host rock, as biogenic CO_2 input is currently almost non-existent. At the bottom of Morgana Cave, a corrosive seepage from a conduit clogged with allogenic sediments indicates a high degree of aggressiveness, acquired through the weathering of pyrite-rich materials (Fig. 17A). In Veronica Cave, it produces extensive boxwork, with very thin blades of Mn oxides (Fig. 17B).

It is difficult to assess the role played by SAS in the formation and development of underground volumes. It probably plays a major role during the inception phase, when the water circulating slowly in the fissures would otherwise be rapidly saturated, and during the late phase, when the small volumes of condensation water can become highly acidic. On the other hand, during the active mature phases, when an abundant water flow circulates rapidly through the conduits, the sulfuric acid produced in small quantities is diluted by meteoric flows, and the impact of this additional acidity is probably negligible.

We should also mention the possibility of an inception associated with circulations of hydrothermal fluids, originating from the Oligocene Masino-Bregaglia pluton. Distant by only a few kilometers to the west and responsible for intense contact metamorphism and metasomatism processes, which are well known in the nearby Val Sissone affecting the Triassic dolomites of Cima di Vazzeda with intrusion of magmatic fluids and subsequent formation of a large variety of minerals (Montrasio, 1991), upward flows in the dolomitic marble may have contributed to an early genesis of hypogene origin. No field evidence has been found to support this hypothesis, but it should not be ruled out.

5.3. Phreatic flow during the mature activity phases

At the maturity of their active phase, the conduits evolved in phreatic regime. Recharge was diffuse or concentrated in sinkholes such as Morgana Cave. Marsooi Cave, located at the base of the dolomitic stripe, functioned as an emergence, as indicated by the ascending tube along a fracture. The resulting morphologies correspond to tubes controlled by foliation planes or fractures (Fig. 13C). The ceilings are sculpted with interlocking cupolas (Fig. 12C), whose origin is attributed to this phreatic phase, as they are oriented along the inclined foliation planes and fractures (those linked to condensation-corrosion develop vertically, independently of any fractures; Barriquand et al., 2021).

Veronica Cave has much larger volumes than Morgana and Marsooi caves (Santagata et al., 2018), hinting to its older age, subjected to a higher number of active phases (i.e. melting and warmer periods), as confirmed by the cosmogenic burial date. This cave might have been activated several times close to the glacial front, whereas the two smaller-sized caves might have formed only during the last glacier retreats. In Morgana Cave, the fracture-controlled steep conduits evolved in epiphreatic conditions, i.e. with flow alternately at free surface and full pipe; they exhibit pseudo-meander morphologies with smooth, rounded walls.

5.4. Vadose flow during the late activity phases of quaternary periglacial environment

Generally speaking, the morphologies produced by torrential flow are few and not very marked, the initial phreatic forms being generally well preserved. The only notable incision is associated with the small stream flowing through Morgana Cave, having produced a shallow 50 cm-deep incision (Fig. 13C). This limited imprint by torrential flows can be explained by a combination of several factors: water from the periglacial environment is not very aggressive, sudden snow-glacial melts produce backflooding where full pipe flow replaces torrential runoff, and lastly, the mobility of the glacial front frequently reorganizes infiltration zones, which at shallow depths are then dispersed and of reduced activity over time.

5.5. Injections of glaciofluvial sediments

Allogenic sediments of glacial origin have been found in the two largest caves. In Veronica Cave, they are limited to a cemented patch of gravels and small pebbles of quartz and metamorphic rocks (samples V1–2-3, burial dated; Fig. 12E). Their horizontal stratification suggests deposition by complete clogging of the conduit, rather than a remnant of terraces brought in by a stream flowing down the steeply sloping gallery. In Morgana Cave, a tributary at the base of the shafts brings small pebbles of calcschist and grey marble. Since quartz is absent, the origin is in fact different from those in Veronica. These pebbles fill lateral pockets all the way down to the bottom (Fig. 13D). In Marsooi Cave, the sediments are fine, due to relatively slow rising water due to backflooding, and are composed of green silts derived from shales. Although these veneered sediments are currently scarce, their distribution shows that Veronica and Morgana were almost entirely filled and then completely emptied, with the exception of a few pockets protected from torrential flows. This sequence of clogging and unclogging probably occurred several times, as small differences in grainsize and erosional surfaces indicate. In Morgana Cave, the recent runoff has produced backflooding which lined the conduit with a coating of black silts resulting from the reworking of ancient fluvio-glacial deposits (Fig. 13C).

5.6. Rarity of speleothems

As in most alpine caves, speleothems are rare. A single calcite deposit has been identified in Veronica Cave, responsible for the cementation - and preservation - of the glacial gravels. In winter conditions, the incoming cold air flow heats up and dries out the cave atmosphere, allowing some minerals to precipitate by evaporation. In Marsooi Cave, which is particularly dry, calcite and aragonite popcorns cover part of the walls (Fig. 13A, B) or form rims around micro-conduits bringing moisture. Some of these coralloids contain traces of vanadinite, which occurs diffusely in dolomitic marble (*P. nana* personal comm.). Gypsum resulting from the oxidation of pyrites develops in the form of needles and crusts (Fig. 13B). In Veronica Cave, gypsum forms crusts around the pyrite inclusions (Fig. 12A). Morgana Cave does not show any evaporitic minerals, due to the wet atmosphere created by the presence of the cascading stream.

5.7. Specific subterranean microclimate causing condensation-corrosion and evaporation

In Veronica Cave, a draught flows through the main conduit between the entrance and the upstream boulder choke, which communicates with the surface. In early winter, the icy, low-moisture, outside air is

sucked in through the entrance, where it warms up and dries out the cave. In summer, the reversal of conditions produces cooling and condensation on the cold walls. Morgana Cave is only slightly ventilated from the outside, but internal runoff maintains a high level of humidity that trickles down the walls. Finally, Marsooi is a confined descending cave. In early winter, an unstable situation allows surface cold air to rush in. This downward airflow gradually heats up and dries out the ground, while the slightly heated return flow rises and cools along the ceilings, forming a condensation-corrosion ceiling channel. In summer, the descending geometry favors the stability of air masses and blocks any air exchange.

In winter, all caves are covered with a more or less thick blanket of snow, so that temperatures of the entering air is stable and is not as cold as the outside temperatures, which are well below 0 °C (Fig. 15).

As a result, winter conditions favor the precipitation of secondary minerals by evaporation (calcite, aragonite, gypsum, hydromagnesite, and possibly dolomite), as mentioned above. Summer conditions, on the other hand, favor condensation, with however some areas remaining dry due to internal convection (Fig. 13A, B). The condensation water, made aggressive by pyrite oxidation, produces particularly corrosive films, at the origin of characteristic "grooved" surfaces (Fig. 12D, F). Condensation mainly occurs along fissures, enlarging them to create these grooved surfaces, whereas the lower portions of the passages are essentially dry due to evaporation; this is where hydromagnesite has been sampled.

In addition to the grooved walls and boxworks mentioned above, the small "Grotta della Cena" displays large flat facets (Fig. 18A). The conduit is an almond-shaped tube, inclined along an oblique foliation plane. Condensation water flowing as a film has uniformly lowered this plane by >15 cm. In the absence of speleothems to date this corrosion plane, it is not possible to quantify the rate of wall retreat. It is assumed, however, that the process is not recent, and may have been operating during several of the last interglacial periods. While this site provides an eloquent illustration of the participation of this late condensation-corrosion process in the morphological evolution of subterranean conduits, we note that it is omnipresent in the caves of the area (smooth wavy walls, condensation-corrosion ceiling channels, grooved surfaces, flat facets, etc.), although we cannot really measure its contribution to the evolution and retreat of the walls. Audra (2000), using the mineralogy of glacial varves in Slovenian Alps, has shown that flow from melting glaciers mainly washed the weathered caves walls that were previously disaggregated by interglacial condensation-corrosion. Considering the age of the Scerscen caves (>1.3 Ma), and even the assumption that the processes were blocked during the Quaternary freeze-up phases, it must be kept in mind that condensation-corrosion was active over periods of several hundreds of thousands of years (probably ca. 250 kyrs), and that it inevitably significantly modified the initial appearance of the walls, giving the wavy aspect. In fact, despite the floods that flowed through the cave passages, scallops are not visible anymore, even though the massive marble bedrock would have been perfectly suited for such sculptures. They were clearly completely erased by later condensation-corrosion. Also rock blocks fallen from ceilings often exhibit smoothed and rounded surfaces, and any trace of detachment surfaces on ceiling is generally lacking: another proof of the efficiency of condensation-corrosion processes over time.

Cave air monitoring has shown different temperatures at different heights in the galleries: condensation processes are in fact much more prone to happen on ceilings and high on the walls, where condensation-corrosion morphologies are more evident (even if corrosion is also observed on the floors). Understanding the energy exchanges of the cave with the outside surface is basic for investigating condensation-corrosion phenomena: these processes are still not completely understood, but are presently considered very important for the evolution of high mountain caves.

5.8. Current hydrogeologic dynamics

The dye tracing experience allowed the identification of the main outflows of the carbonate aquifer at La Prediletta Spring (C2). The calculated flow velocity (> 20 m/h) is typical of a highly karstified aquifer, with large drains, however combined with dispersive flow through fracture permeability, as evidenced by the slow restitution recorded in C1 spring. This behavior is consistent with the coldest temperatures (2.2 to 3.7 °C) and EC in the range of 170–190 μS/cm, typical of rather short residence time.

As expected, the karst aquifer discharges at the lowest outcropping site, at the foot of the dolomitic marble ridge, along the Lanterna valley (Figs. 7, 19). According to the complex folded structure, we suggest the presence of a saturated zone in the core of the syncline, whose depth is not known.

6. Conclusions

The Scerscen caves are currently located at the edge of the glacier at about 2600 m asl. In this paper, we described a long evolution, starting long before glaciations (Fig. 20).

- In Veronica Cave, the ages of the quartz pebbles it contains have been dated to 1.3 ± 0.4 Ma for some, with others possibly older than 1.5 Ma, meaning that the cave is even older. Given the age of its filling and the average uplift rate, it must have developed at a lower altitude, around 1300 ± 200 m asl or lower. At this altitude and during this period, the environment allowed the development of a vegetation cover, providing the necessary aggressiveness for karstification. The inception phases may have been facilitated by sulfuric acid speleogenesis (SAS) corrosion, thanks to the oxidation of pyrite contained in the marbles. The conduits, which mainly function as phreatic flow, have inherited tube-like morphologies.
- During the Pleistocene, gradual uplift brought the karst to higher altitudes. It was then alternately covered by ice during glaciations with seasonal drainage of snowmelt and glacial meltwater, and on the edge of glaciers during interglacial periods. The smaller caves might have formed in some of these warmer periods, when enough vegetation and soil, and thus CO_2, was available near and above the caves.
- Currently, and since the end of the Little Ice Age (LIA), the caves are slowly evolving. The flow of the stream in Morgana gradually clears the coarse fill, with backflooding during seasonal floods, making a shallow incision. For all caves, the humidity from seepage and condensation acidified by the oxidation of pyrite from the surrounding rock and sedimentary fills contributes significantly to enlargement. The effect of condensation-corrosion has produced a wall retreat measured at 15 cm in Grotta della Cena Cave. Although not quantifiable elsewhere, it is responsible for the morphologies of smooth wavy walls, flat facets, grooved surfaces, and condensation-corrosion ceiling channels.

- Tracing has made it possible to characterize the current flows, mainly drained by the Prediletta spring, located in the Lanterna valley, at the lowest point of the carbonate aquifer, and in contact with the less permeable bedrock. Circulation velocities (> 20 m/h), very low temperatures (≈ 2 °C), and conductivity (around 200 μS/cm for concentrated flows and 300–400 μS/cm for slow seepage), are indicative of a generally well-organized karst aquifer that promotes rapid transfers, accompanied with a slower circulation through a fracture network.
- The current periglacial environment, and glacial environment during previous periods, is not favorable for calcite deposition. The only speleothems identified are calcite-aragonite popcorns, gypsum crusts, and hydromagnesite clusters, located only in the rare spots where evaporation allows for their deposition.

- Temperature (T) and humidity (RH) records show that humidity is at saturation most of the time, especially when exchanges with the outside are blocked by thick snow cover. However, outside of winter, airflow activates when the entrances reopen after gradual snow melting, and when sudden atmospheric cooling occurs, the airflow in Veronica and Marsooi warms up and dries out. Humidity sometimes drops down to 50–65 %, causing intense evaporation and the possibility of speleothems to form (calcite-aragonite popcorns, hydromagnesite, gypsum crusts).

We have demonstrated that the Scerscen caves, located at very high altitude on the edge of the glacier, were formed in part before the ice ages and have continued to evolve since then through filling-clearing and condensation-corrosion. The study of microclimatic records might provide a better understanding of energy flows and condensation/evaporation cycles.

Supplementary data to this article can be found online at https://doi.org/10.1016/j.geomorph.2025.110054.

CRediT authorship contribution statement

Philippe Audra: Writing – original draft, Visualization, Validation, Methodology, Investigation, Formal analysis, Data curation, Conceptualization. **Jo De Waele:** Writing – original draft, Validation, Methodology, Investigation, Data curation, Conceptualization. **Alessandro Uggeri:** Visualization, Validation, Methodology, Investigation, Formal analysis, Data curation. **Didier Cailhol:** Visualization, Validation, Methodology, Investigation, Formal analysis, Data curation. **Ilenia M. D'Angeli:** Methodology, Investigation, Formal analysis, Data curation. **Adriano Fiorucci:** Visualization, Validation, Methodology, Formal analysis, Data curation. **Ivano Foianini:** Investigation. **Samuele Foianini:** Investigation. **Régis Braucher:** Validation, Methodology, Investigation, Formal analysis, Data curation. **Mauro Inglese:** Visualization, Investigation. **Andrea Maconi:** Investigation. **Felicita Spreafico:** Investigation. **Marco Barile:** Investigation. **Cristina Carbone:** Visualization, Methodology, Investigation, Formal analysis, Data curation. **Paola Tognini:** Writing – original draft, Visualization, Validation, Supervision, Resources, Project administration, Methodology, Investigation, Funding acquisition, Formal analysis, Data curation, Conceptualization.

Declaration of competing interest

The authors declare that they have no known competing financial interests or personal relationships that could have appeared to influence the work reported in this paper.

Acknowledgements

This project was part of the Italian-Swiss Interreg Project - Progetto B-ICE & Heritage "Bernina Terra Glacialis", in collaboration with the Municipality of Lanzada, the "Comunità Montana" of Sondrio, the Union of Municipalities of Valmalenco, the BIM (Bacino Imbrifero Montano dell'Adda), the Province of Sondrio, and the Institute of Mineralogy of Valtellina; Sondrio Rotary Club funded the first phase of the investigation program. Cavers of the Lombard Speleological Federation made all exploration and mapping activities possible. Technical support came from Leica Geosystems and VIGEA-Virtual Geographic Agency (Reggio Emilia) (thanks to Tommaso Santagata), while Elitellina Helicopter Services ensured helicopter flights. Cosmonucleide dating was performed at ASTER AMS, national facility (CEREGE, Aix-en-Provence), which is supported by the INSU/CNRS and IRD, and member of Aix-Marseille Platforms and REGEF networks. We also thank Giorgio Tomasi (Gruppo Speleologico Valseriana) for producing videos of all the investigation phases, Marco Marchesini for his passionate stories about Valtellina's mineralogical heritage, Claudia Canedoli and Davide Corengia of the Gruppo Grotte CAI Saronno for help during fieldwork, Alfredo Corti and Fabiano Ventura, and especially the "Associazione Macromicro", for the permission to use the historical pictures of Scerscen Glacier, and Luca Pisani for the petrographic thin section analyses.

Data availability

Data will be made available on request.

References

Audra, P., 2000. Le karst haut alpin du Kanin (Alpes juliennes, Slovénie-Italie). État des connaissances et données récentes sur le fonctionnement actuel et l'évolution plio-quaternaire des structures karstiques. Karstologia 35, 27–38 https://www.persee.fr/doc/karst_0751-7688_2000_num_35_1_2456.

Audra, P., 2004. Kitzsteinhorn high-alpine karst (Salzburg, Austria): evidence of non-glacial speleogenesis. Die Höhle 55 (1–4), 12–18. https://www.zobodat.at/pdf/Hoehle_055_0012-0018.pdf.

Audra, P., Bini, A., Gabrovšek, F., Häuselmann, P., Hobléa, F., Jeannin, P.Y., Kunaver, J., Monbaron, M., Šušteršič, F., Tognini, P., Trimmel, H., Wildberger, A., 2006. Cave genesis in the Alps between the Miocene and today: a review. Z. Geomorphol. 50 (2), 153–176. https://doi.org/10.1127/zfg/50/2006/153.

Audra, P., Gázquez, F., Rull, F., Bigot, J.-Y., Camus, H., 2015. Hypogene Sulfuric Acid Speleogenesis and rare sulfate minerals in Baume Galinière Cave (Alpes-de-Haute-Provence, France). Record of uplift correlative cover retreat and valley dissection. Geomorphology 247, 25–34. https://doi.org/10.1016/j.geomorph.2015.03.031.

Auler, A.S., Smart, P.L., 2003. The influence of bedrock-derived acidity in the development of surface and underground karst: evidence from the Precambrian carbonates of semi-arid northeastern Brazil. Earth Surf. Process. Landf. 28 (2), 157–168. https://doi.org/10.1002/esp.443.

Barriquand, L., Bigot, J.-Y., Audra, P., Cailhol, D., Gauchon, C., Heresanu, V., Jaillet, S., Vanara, N., 2021. Caves and Bats: morphological impacts and archaeological consequences. The Azé Prehistoric Cave (Saône-et-Loire, France). Geomorphology 388, 107785. https://doi.org/10.1016/j.geomorph.2021.107785.

Beniston, M., Farinotti, D., Stoffel, M., Andreassen, L.M., Coppola, E., Eckert, N., Fantini, A., Giacona, F., Hauck, C., Huss, M., Huwald, H., Lehning, M., López-Moreno, J.-I., Magnusson, J., Marty, C., Morán-Tejéda, E., Morin, S., Naaim, M., Provenzale, A., Rabatel, A., Six, D., Stötter, J., Strasser, U., Terzago, S., Vincent, C., 2018. The European mountain cryosphere: a review of its current state, trends, and future challenges. Cryosphere 12 (2), 759–794. https://doi.org/10.5194/tc-12-759-2018.

Bonardi, L., Rovelli, E., Scotti, R., Toffaletti, A., Urso, M., Villa, F., 2012. I ghiacciai della Lombardia – evoluzione e attualità. Servizio Glaciologico Lombardo, Hoepli, p. 328.

Calvet, M., Gunnell, Y., Delmas, M., Braucher, R., Jaillet, S., Häuselmann, P., Delunel, R., Sorriaux, P., Valla, P.G., Audra, P., 2024. Valley incision chronologies from alluvium-filled cave systems. Earth Sci. Rev. 258, 104963. https://doi.org/10.1016/j.earscirev.2024.104963.

Chmeleff, J., von Blanckenburg, F., Kossert, K., Jakob, D., 2010. Determination of the ^{10}Be half-life by multicollector ICP-MS and liquid scintillation counting. Nuclear Instruments and Methods B 268, 192–199. https://doi.org/10.1016/j.nimb.2009.09.012.

Corbel, J., 1957. Les karsts du nord-ouest de l'Europe. Mémoires et Documents de l'Institut des études Rhodaniennes 12, 541.

Cornwall, C.E., Comeau, S., Kornder, N.A., Perry, C.T., van Hooidonk, R., DeCarlo, T.M., Pratchett, M.S., Anderson, K.D., Brownem, N., Carpenter, R., Diaz-Pulido, G., D'Olivo, J.P., Doo, S.S., Figueire, J., Fortunato, S.A.V., Kennedy, E., Lantz, C.A., McCulloch, M.T., González-Rivero, M., Schoepf, V., Smith, S.G., Lowe, R.J., 2021. Global declines in coral reef calcium carbonate production under ocean acidification and warming. Proc. Natl. Acad. Sci. 118 (21). https://doi.org/10.1073/pnas.2015265118.

De Waele, J., D'Angeli, I.M., Audra, P., Plan, L., Palmer, A.N., 2024. Sulfuric acid caves of the world: a review. Earth Science Review 104693, 1–30. https://doi.org/10.1016/j.earscirev.2024.104693.

De Waele, J., Shen, C.C., Vigna, B., Fiorucci, A., Marini, P., Huang, C.Y., Hu, H.M., 2025. Speleogenesis of Valdemino Cave (Borgio Verezzi, Liguria, Northern Italy) shows very slow uplift of this coast since middle Pleistocene. Geomorphology, 109636. https://doi.org/10.1016/j.geomorph.2025.109636.

Diffenbaugh, N.S., Singh, D., Mankin, J.S., Horton, D.E., Swain, D.L., Touma, D., Charland, A., Liua, Y., Haugen, M., Tsiang, M., Rajaratnam, B., 2017. Quantifying the influence of global warming on unprecedented extreme climate events. Proc. Natl. Acad. Sci. 114 (19), 4881–4886. https://doi.org/10.1073/pnas.161808211.

Dioli, P., Foianini, I., Tognini, P., 2012. Presenza dell'opilionide calcifilo *Dicranopalpus gasteinensis* Doleschal, 1852 (Aracnida, Opiliones, Phalangidae) nelle grotte della Valmalenco (Provincia di Sondrio, Lombardia, Italia settentrionale). Il Naturalista Valtellinese, Atti Musei Civico di Storia Naturale di Morbegno 23, 5–14. https://www.museostorianaturale.it/site/assets/files/1054/2012_23_5-14_dioli.pdf.

Galliano, Y., Carbone, C., Balestra, V., Belmonte, D., De Waele, J., 2022. Secondary minerals from minothem environments in Fragnè Mine (Turin, Italy): preliminary results. Minerals 12 (8), 966. https://doi.org/10.3390/min12080966.

Galluccio, A., Scotti, R., 2022. Storia recente del Ghiacciaio di Scerscen (Bernina italiano). Relazione, 24 p.. https://www.researchgate.net/publication/362091796.

Granger, D.E., Muzikar, P.F., 2001. Dating sediment burial with in-situ produced cosmogenic nuclides: theory, techniques, and limitations. Earth Planet. Sci. Lett. 188. https://doi.org/10.1016/S0012-821X(01)00309-0, 269–28.

Hansen, J.E., Sato, M., Simons, L., Nazarenko, L.S., Sangha, I., Kharecha, P., Zachos, J.C., von Schuckmann, K., Loeb, N.G., Osman, M.B., Jin, Q., Tselioudis, G., Jeong, E., Lacis, A., Ruedy, R., Russell, G., Cao, J., Li, J., 2023. Global warming in the pipeline. Oxf. Open Clim. Change 3 (1). https://doi.org/10.1093/oxfclm/kgad008.

Heeb, B., 2014. The next generation of the DistoX Cave surveying instrument. CREG J. 88, 5–8.

Hill, C., Forti, P., 1997. Cave Minerals of the World. National Speleological Society, Huntsville, p. 463.

Horn, G., 1935. Über die Bildung von Karsthöhlen unter einem Gletcher. Nor. Geogr. Tidsskr. 5, 494–498. https://doi.org/10.1080/00291953508542704.

Horn, G., 1978. Limestone caves in Nordland. Cave Geol. 1 (5), 124–138.

Hugonnet, R., McNabb, R., Berthier, E., Menounos, B., Nuth, C., Girod, L., Farinotti, D., Huss, M., Dussaillant, I., Brun, F., Kääb, A., 2021. Accelerated global glacier mass loss in the early twenty-first century. Nature 592, 726–731. https://doi.org/10.1038/s41586-021-03436-z.

Jurado, V., Gonzalez-Pimentel, J.L., Miller, A.Z., Hermosin, B., D'Angeli, I.M., Tognini, P., De Waele, J., Saiz-Jimenez, C., 2020. Microbial communities in vermiculation deposits from an Alpine cave. Front. Earth Sci. 8, 586248. https://doi.org/10.3389/feart.2020.586248.

Korschinek, G., Bergmaier, A., Faestermann, T., Gerstmann, U.C., Knie, K., Rugel, G., Wallner, A., Dillmann, I., Dollinger, G., Lierse von Gostomski, Ch., Kossert, K., Maiti, M., Poutivtsev, M., Remmert, A., 2010. A new value for the half-life of ^{10}Be by Heavy-Ion Elastic Recoil Detection and liquid scintillation counting. Nuclear Instruments and Methods B 268, 187–191. https://doi.org/10.1016/j.nimb.2009.09.020.

Lauritzen, S.E., 1986. Kvithola at Fauske; Northern Norway: an example of ice-contact speleogenesis. Nor. Geol. Tidsskr. 66 (2), 153–161. https://njg.geologi.no/images/NJG_articles/NGT_66_2_153-161.pdf.

Lauritzen, S.E., 2001. Marble stripe karst of the Scandinavian Caledonides. Acta Carsolog. 30 (2), 47–79. https://www.dlib.si/details/URN:NBN:SI:doc-CWIDV4EP.

Lauritzen, S.E., Gascoyne, M., 1980. The first radiometric dating of Norwegian stalagmites; evidence of pre-Weichselian karst caves. Nor. Geogr. Tidsskr. 34, 77–82. https://doi.org/10.1080/00291958008621917.

Lauritzen, S.E., Skoglund, R.Ø., 2013. Glacier ice-contact speleogenesis in marble stripe karst. In: Frumkin, A. (Ed.), Treatise in Geomorphology, 6. Elsevier, pp. 363–396. https://doi.org/10.1016/B978-0-12-374739-6.00111-1.

Montrasio, A., 1991. Valmalenco, itinerario n. 10. In: Cita, M., Gelati, R., Gregnanin, A. (Eds.), Alpi e Prealpi Lombarde. Guide Geologiche Regionali, 1. Società Geologica Italiana, BE-MA Ed., pp. 262–264

Montrasio, A., Trommsdorff, V., Hermann, J., Müntener, O., Spillmamm, P., 2004. Carta Geologica della Valmalenco alla scala 1:25,000. Quaderni di Geodinamica Alpina e Quaternaria, 8, Istituto per la Dinamica dei Processi Ambientali, CNR, Milano, 16 p.

Muttoni, G., Carcano, C., Garzanti, E., Ghielmi, M., Piccin, A., Pini, R., Rogledi, S., Sciunnach, D., 2003. Onset of major Pleistocene glaciations in the Alps. Geology 31 (11), 989–992. https://doi.org/10.1130/G19445.1.

Norris, T.L., Gancarz, A.J., Rokop, D.J., Thomas, K.W., 1983. Half-life of ^{26}Al. J. Geophys. Res. Solid Earth 88 (S01), B331–B333. https://doi.org/10.1029/JB088iS01p0B331.

Pepin, N., Arnone, E., Gobiet, A., Haslinger, K., Kotlarski, S., Notarnicola, C., Palazzi, E., Seibert, P., Serafin, S., Schöner, W., Terzago, S., Thornton, J.M., Vuille, M., Adler, C., 2022. Climate changes and their elevational patterns in the mountains of the world. Rev. Geophys. 60 (1). https://doi.org/10.1029/2020RG000730.

Santagata, T., De Waele, J., D'Angeli, I.M., Foianini, I., Audra, P., Cailhol, D., Tognini, P., 2018. Laser Scanning and 3D Mobile Mapping of High-Altitude Caves in Valmalenco (Lombardia, Italy). Proceeding of the 19th Eurospeleo Forum, Ebensee (Austria), 110 (Abstract). In: https://www.academia.edu/37556534/Proceedings_of_the_12th_EuroSpeleo_Forum_Austria_2018.

Sauro, F., Fellin, M.G., Columbu, A., Häuselmann, P., Borsato, A., Carbone, C., De Waele, J., 2021. Hints on the late Miocene evolution of the Tonale-Adamello-Brenta region (Alps, Italy), based on allochtonous sediments from Raponzolo Cave. Front. Earth Sci. 9, 672119. https://doi.org/10.3389/feart.2021.672119.

Skoglund, R.Ø., Lauritzen, S.E., 2010. Morphology and speleogenesis of Okshola (Fauske, northern Norway): example of a multi-stage network cave in a glacial landscape. Nor. J. Geol. 90, 123–139. https://njg.geologi.no/images/NJG_articles/NJG_3_2010_Skoglund_hoy.pdf.

Skoglund, R.Ø., Lauritzen, S.E., Gabrovšek, F., 2010. The impact of glacier ice-contact and subglacial hydrochemistry on evolution of maze caves: a modelling approach. J. Hydrol. 388 (1–2), 157–172. https://doi.org/10.1016/j.jhydrol.2010.04.037.

Sommer, C., Malz, P., Seehaus, T.C., Lippl, S., Zemp, M., Braun, M.H., 2020. Rapid glacier retreat and downwasting throughout the European Alps in the early 21st century. Nat. Commun. 11 (1), 3209. https://doi.org/10.1038/s41467-020-16818-0.

Spötl, C., Mangini, A., 2010. Paleohydrology of a high-elevation, glacier-influenced karst system in the Central Alps (Austria). Austrian J. Earth Sci. 103 (2), 92–105. https://www.zobodat.at/publikation_articles.php?id=173738.

Sternai, P., Sue, C., Husson, L., Serpelloni, E., Becker, T.W., Willett, S.D., Faccenna, C., Di Giulio, A., Spada, G., Jolivet, L., Valla, P., Petit, C., Nocquet, J.-M., Walpersdorf, A., Castelltort, S., 2019. Present-day uplift of the European Alps: evaluating mechanisms and models of their relative contributions. Earth Sci. Rev. 190, 589–604. https://doi.org/10.1016/j.earscirev.2019.01.005.

Tognini, P., D'Angeli, I.M., Santagata, T., De Waele, J., 2017. Progetto grotte della Val di Scerscen. Speleologia 77, 36–37. https://www.speleo.it/site/images/speleologia/Speleologia_77_Dic_2017.pdf.

Tognini, P., Canedoli, C., De Waele, J., Inglese, M., Maconi, A., Spreafico, F., Uggeri, A., 2024. Ai piedi del ghiacciaio: le grotte della Val di Scerscen. Speleologia 89, 46–52. https://www.speleologiassi.it/89-scerscen/.

Valla, P.G., Shuster, D.L., Van Der Beek, P.A., 2011. Significant increase in relief of the European Alps during mid-Pleistocene glaciations. Nat. Geosci. 4 (10), 688–692. https://doi.org/10.1038/ngeo1242.

Višnjević, V., Herman, F., Prasicek, G., 2020. Climatic patterns over the European Alps during the LGM derived from inversion of the paleo-ice extent. Earth Planet. Sci. Lett. 538, 116185. https://doi.org/10.1016/j.epsl.2020.116185.

Webb, J.A., 2021. Supergene sulphuric acid speleogenesis and the origin of hypogene caves: evidence from the Northern Pennines. UK. Earth Surface Processes and Landforms 46 (2), 455–464. https://doi.org/10.1002/esp.5037.